Why is Most Neurotransmitter Release Synaptic?

by

Abigail J. LeBlanc

Submitted in partial fulfillment of the requirements
for the degree of Master of Science

at

Dalhousie University
Halifax, Nova Scotia
April, 2024

Dalhousie University is located in Mi'kma'ki, the
ancestral and unceded territory of the Mik'kmaq.
We are all Treaty people.

TABLE OF CONTENTS

LIST OF FIGURES

ABSTRACT

Small-molecule neurotransmitter release is largely confined to synaptic active zones, but the spatially restrictive mechanism is unidentified. In this study, we investigate whether spatial restriction occurs during synaptic vesicle fusion with the plasma membrane or the priming stage where synaptic vesicles are attached to the plasma membrane. Calcium concentrations that activate low-affinity sensors like Syt-1 are achieved only at VGCCs that localize to active zones which may spatially restrict release. We hypothesize that spatial restriction can be overcome by high-affinity calcium sensors. Alternatively, restriction may occur during priming, which involves the formation of a complex of proteins located on synaptic vesicles and plasma membranes. A protein catalyzing this process, Munc13-1, is recruited and activated by the active zone protein RIM. This interaction may also cause release's spatial confinement. Our cellular-imaging experiments utilizing a genetically encoded exocytosis sensor favors spatial restriction during priming. Additional work is necessary to resolve the question.

LIST OF ABBREVIATIONS USED

ΔF	Fluorescence increase
Bsn	Bassoon
DCV	Dense core vesicles
DKO	Double Knockout
Doc2	Double C2-like domain containing
KD	Knockdown
KO	Knockout
MUNC	Mammalian uncoordinated
OE	Overexpression
RIM	Rab-interacting molecule
RIM-BP	Rab-interacting molecule binding protein
SNARE	Soluble NSF attachment protein receptor
SypH	Synaptophysin-pHluorin
Syt	Synaptotagmin
tdT	tdTomato
UNC	uncoordinated
VGCC	Voltage-gated calcium channel

CHAPTER 1: INTRODUCTION

The release of small molecule neurotransmitters is a highly controlled system to ensure precision and effective neuronal communication. Small molecule neurotransmitter release occurs at specialized sites known as the pre-synaptic active zones. The active zone is distinct along axonal segments due to the presence of cytomatrix proteins including bassoon (Bsn) and piccolo (Dieck et al., 1998; Garner et al., 2000; Hallermann et al., 2010; Mukherjee et al., 2010). Active zone cytomatrix and associated proteins are thought to comprise an extensive network that functions to prepare the synaptic vesicle for exocytosis. This preparation occurs in three defined steps: docking, priming, and fusion.

Defined Steps of Synaptic Vesicle Exocytosis

Synaptic Vesicle Docking

The first step, docking, is thought to be responsible for carrying out the tethering of synaptic vesicles to the active zone plasma membrane in proximity to voltage-gated calcium channels (VGCCs), which are concentrated at presynaptic active zones (Kaeser et al., 2011; Holderith et al., 2012). Synaptic vesicles need to be closely associated with VGCCs to quickly respond to the influx of calcium following the arrival of an action potential, as outlined later. To accomplish this task, the protein Rab3-interacting molecule (RIM) recruits and forms a complex with an accessory RIM-Binding Protein (RIM-BP) at RIM's PxxP-site (Y. Wang et al., 2000; Acuna et al., 2015, 2016); see also Figure 1.1. Together RIM and RIM-BP interact with VGCCs through RIM's PDZ-domain (Kaeser et al., 2011) and RIM-BP's SH3 domain (Y. Wang et al., 2000; Hibino

et al., 2002). In addition to the association that RIM makes with VGCCs, RIMs Zn-finger domain binds to a Rab3 family protein located on the synaptic vesicle membrane (Wang et al., 1997).

This RIM-mediated interaction is crucial for the vesicle to achieve docking. Neurons lacking the expression of all RIM proteins experience a significant decrease in docked synaptic vesicles (Kaeser et al., 2011; Acuna et al., 2016). However, during RIM knockout (KO) experiments, some vesicles are still able to dock to the plasma membrane suggesting some other protein may compensate in the absence of RIM. Another family of proteins, ELKS, likely function similarly to RIMs by tethering synaptic vesicles to the plasma membrane and compensates when RIM proteins are not available (Ohtsuka et al., 2002; Deken, 2005; Liu et al., 2014; Held & Kaeser, 2018). The KO of ELKS proteins by themselves reduces, but does not eliminate, synaptic vesicle docking and neurotransmitter release (Held et al., 2016). Once both RIM and ELKS are knocked-out together (DKO) a complete loss of docked vesicles occurs, in addition to a strong reduction of other active zone cytomatrix proteins such as Bsn and piccolo (Wang et al., 2016; Tan et al., 2022). The result of RIM and ELKS DKO is greater than the sum of the individual effects of a single KO of either protein. Surprisingly, neurotransmitter release is not abolished in the absence of docked synaptic vesicles. In neurons devoid of RIM and ELKS proteins, synaptic vesicle docking, as assessed by electron microscopy, is severely diminished. In these neurons, synaptic transmission evoked by isolated action potentials is strongly reduced. However, a pool of readily releasable synaptic vesicles remains, and high-frequency trains of action potentials can still elicit substantial synaptic transmission (Wang et al., 2016; Tan et al., 2022). These findings suggest that synaptic vesicle docking to active zones is not strictly required for neurotransmitter release. Rather, it appears that docking is required for

tight spatial coupling of synaptic vesicles to VGCCs to allow for efficient and temporally precise neurotransmitter release (Tan et al., 2022).

Synaptic Vesicle Priming

The second step for neurotransmitter release is referred to as synaptic vesicle priming (see Figure 1.1B). This phase leads to the formation of the Soluble NSF Attachment Protein Receptor (SNARE) complex which brings the synaptic vesicle into a tight apposition with the active zone plasma membrane in preparation for vesicle fusion. The SNARE complex is comprised of two plasma membrane proteins, syntaxin and SNAP-25, and the synaptic vesicle protein synaptobrevin (Rizo & Xu, 2015). Before priming occurs, the three SNARE complex proteins are found in inactive states that require assistance from two proteins, Uncoordinated-13 (Unc-13, in mammals called Munc-13) and Uncoordinated-18 (Unc-18, or Munc-18 in mammals). Together, Munc-13 and Munc-18 interact with the unbound SNARE proteins to mediate the formation of the complex (Rizo & Xu, 2015). Munc-18 is a member of the Sec1/Munc18 (SM) protein family that, like the SNARES, has a critical role in membrane fusion during neurotransmitter release as well as in most types of intracellular membrane traffic. It has been shown to bind to syntaxin, possibly to stabilize syntaxin's expression at the plasma membrane (Toonen et al., 2005; Zilly et al., 2006; Diao et al., 2010; Kasai et al., 2012) and/or to promote, possibly in concert with Munc13, a conformational change of syntaxin that renders it competent for SNARE complex formation (Han et al., 2013; Martin et al., 2013) Although Munc-18's role in priming is still under investigation, it is established that Munc-18 is required for all forms of vesicle exocytosis, as the loss of Munc-18 has been shown to lead to the complete abolition of both evoked and spontaneous neurotransmitter release (Verhage et al., 2000). It is

suggested that Munc-18 facilitates the interaction between syntaxin and SNAP-25 which can then finalize the SNARE complex through the binding of synaptobrevin (Pevsner et al., 1994; Zilly et al., 2006; Y. Xu et al., 2010).

Unc-13/Munc-13, structurally unrelated to Munc-18, is another protein that binds to syntaxin. Through an interaction between Munc-13s MUN-domain, syntaxin undergoes a conformational change to an active state in which it is capable of binding to SNAP-25 and Synaptobrevin (Brose et al., 1995; Richmond et al., 2001; Basu et al., 2005; Stevens et al., 2005; Yang et al., 2015). Without the assistance of Munc-13, syntaxin remains in a closed state, and synaptic vesicle priming and eventual vesicle exocytosis is arrested (Augustin et al., 1999; Varoqueaux et al., 2002; Gerber et al., 2008; Yang et al., 2015). This requirement for Munc-13 to activate syntaxin has been shown in C. elegans in which a mutant form of syntaxin causes the protein to be in an open-state that could restore synaptic vesicle exocytosis in the absence of Unc-13. In contrast, an unmutated form of syntaxin was incapable of restoring synaptic vesicle exocytosis without the assistance of Unc-13 (Richmond et al., 2001).

Interestingly, expression of the open-form of syntaxin does not overcome the reliance of neurotransmitter release on Unc-18, suggesting that Unc-18 has other or additional functions (Weimer et al., 2003). The requirement of Munc-13 and Munc-18 for neurotransmitter release, along with evidence that KO (Schoch et al., 2001; Vardar et al., 2016) or enzymatic cleavage (Schiavo et al., 1992; Blasi et al., 1993a; Blasi et al., 1993b) of the SNARE proteins syntaxin, SNAP-25 or synaptobrevin abolishes neurotransmitter release demonstrates that synaptic vesicle priming is a required step in the vesicular release of neurotransmitter.

Synaptic Vesicle Fusion: Synaptotagmin-1 & Synchronous Release

The final step for synaptic vesicle exocytosis is vesicle fusion (see Figure 1.1C). During this stage, primed synaptic vesicles are prompted to fuse with the plasma membrane and expel their content into the synaptic cleft when an action potential invades the presynaptic active zone. The action potential elicits the opening of VGCCs, allowing for an influx of calcium ions into the presynaptic specialization. Calcium ions are detected by specialized calcium sensors located either on the exterior of the synaptic vesicle membrane or at the plasma membrane. Calcium sensors for neurotransmitter release typically belong to the synaptotagmin (Syt) protein family (Sugita et al., 2002). Many isoforms of Syt exist with unique characteristics, but those that detect calcium influx contain two so-called C2 domains (Chapman et al., 1996; Mackler et al., 2002; Stevens & Sullivan, 2003; Chang et al., 2018), calcium-binding domains that also occur in other proteins such as protein kinase C. The event of calcium binding to the C-terminal domain allows Syt to then interact, via its C2 domains, with phospholipids in the plasma membrane and synaptic vesicle membrane, and to facilitate the fusion of these membranes, eliciting neurotransmitter exocytosis (Chapman et al., 1995).

The Syt-isoforms Syt-1, Syt-2, and Syt-9 exhibit a low calcium affinity that requires a calcium concentration between 10-30 μM. These low-affinity Syt isoforms are present on the exterior of the synaptic vesicle plasma membrane (Südhof, 2012) and bind to assembled SNARE complexes. Due to the resulting proximity of synaptic vesicle membrane and plasma membrane, they are able to respond quickly to calcium influx and as such are implicated in synchronous modes of release (Pinheiro et al., 2016). Synchronous release refers to synaptic vesicle exocytosis that is directly paired to the arrival of an action potential (Sugita et al., 2002;

J. Xu et al., 2007; Yoshihara et al., 2010; Bacaj et al., 2013; Turecek & Regehr, 2019). Of note, synaptic vesicle exocytosis elicited by low-affinity calcium sensors only occurs immediately following the action potential, as calcium concentrations required for their activation are only reached as VGCCs in very close proximity to the sensor are open. Within the hippocampus, Syt-1 is the only expressed low-affinity calcium sensor.

Fusion Sensors with Higher Calcium Affinity & Asynchronous Release

Another Syt isoform, Syt-7, has a high calcium affinity requiring concentration between 1-2 μM, but is slow-acting (Sugita et al., 2002) and is associated with an alternative mode release known as asynchronous release (Bacaj et al., 2013; Turecek & Regehr, 2019). This mode of release responds to an action potential over a greater duration of time, within 10 to hundreds of milliseconds, following calcium influx (Kaeser & Regehr, 2014). In most neurons, including hippocampal glutamatergic and GABAergic neurons, both high- and low-affinity Syt isoforms are expressed and both synchronous and asynchronous modes of release are observed. In cases such as hippocampal neurons where both Syt-1 and Syt-7 are present, the asynchronous component of release can only be visualized with high-frequency stimulation events as they elicit longer-lasting increases in presynaptic calcium concentrations. In contrast, asynchronous components of release are largely absent in low-frequency stimulation. Some specialized areas in the brain express only one Syt-isoform and utilize its corresponding mode of release. These distinct regions have provided insight into how the Syt-isoforms expressed influence the mode of neurotransmitter release used.

Within the inferior olive of the medulla oblongata, some nuclei receive GABAergic afferents that only employ asynchronous release (Turecek & Regehr, 2019). Interestingly,

neurons providing these afferents only express synaptotagmin-7, but no low-affinity synaptotagmins, and the overexpression of Syt-1 in these neurons switches their release from asynchronous to synchronous (Turecek & Regehr, 2019). In fact, it is well established that eliminating Syt-1 expression in neurons with both low- and high-affinity calcium sensors will shift release from synchronous to asynchronous release (DiAntonio & Schwarz, 1994; Geppert et al., 1994; J. Xu et al., 2007; Bacaj et al., 2013; Chen et al., 2017). For instance, in Syt-1 knock-out conditions, asynchronous release not only persists but becomes more pronounced (Geppert et al., 1994). This suggests that low-affinity calcium sensors are typically favored when both low- and high-affinity calcium sensors are present, and only once removed can high-affinity calcium sensors come into full effect.

Interestingly, Turecek and Regehr (2019) also found a unique effect of knocking out Syt-7. In nuclei that solely expressed Syt-7, the removal of Syt-7 expression exhibited asynchronous release with even slower kinetics. This suggests that another calcium sensor exists in the absence of Syt-7 with perhaps an even greater calcium affinity. In addition to Syts, other proteins have been considered as potential calcium sensors. One family that has been implicated in calcium-dependent release is the Double C2-like domain containing (Doc2) protein family. In hippocampal neurons, the isoforms Doc2α and Doc2β are co-expressed equally with about 10-fold less expression than Syt-isoforms (Bacaj et al., 2013). Doc2 proteins contain C2-domains that are similar to Syts (Groffen et al., 2006; Friedrich et al., 2008; Groffen et al., 2010; Yao et al., 2011; Pinheiro et al., 2016; Bacaj et al., 2013). Doc2 proteins bind calcium ions with an even greater affinity than Syt-7 at 0.5-1 μM of calcium (A. J. A. Groffen et al., 2004). Evidence also supports that Doc2 proteins interact with the SNARE complex (Groffen

et al., 2010) and Munc-13 (Orita et al., 1997; Mochida et al., 1998). However, the role of Doc2 proteins in neurotransmitter release is still largely debated in the literature. While some have pointed to Doc2-proteins playing a role in asynchronous release (Yao et al., 2011; Bacaj et al., 2013), others suggest Doc2 is involved in an action potential-independent release known as spontaneous release (Groffen et al., 2010; Pang et al., 2011). Spontaneous release differs from asynchronous release as asynchronous release is still paired with an action potential. However, at least some of the spontaneous release is calcium-dependent (Groffen et al., 2010), and it is conceivable that the reported participation of Doc2 in asynchronous and spontaneous release represents two aspects of the same function.

Spatial Restriction of Neurotransmitter Release: Apparent Differences between Neurotransmitter Systems

Neurotransmitter release is largely restricted to the active zone. This spatial restriction allows a targeted exocytosis of neurotransmitter into the synaptic cleft that ensures that the released neurotransmitter efficiently activates the postsynaptically located neurotransmitter receptors which frequently exhibit a low binding affinity for their ligands. Despite this apparent beneficial arrangement, some forms of neuronal communication are elicited by neurotransmitter exocytosis outside of the confinement of active zones and synapses. This type of release is referred to as extrasynaptic release and has been best demonstrated for neuropeptides and monoamines (Bunin & Wightman, 1998; Trueta & De-Miguel, 2012; De-Miguel et al., 2021).

Dense core vesicles (DCV) for neuropeptide release are shown to have no preference for the presynaptic specializations and instead localize anywhere (reviewed in van den Pol, 2012). These DCV are often only released following high-frequency stimulation as they require a greater cytoplasmic calcium concentration than what can be achieved in isolated action potentials (Tallant, 2008; van den Pol, 2012). As such, neuropeptides act in paracrine signaling often called volume transmission, activating receptors away from the site of release on nearby neurons and glial cells (Fuxe et al., 2012; van den Pol, 2012). Receptors for neuropeptides have a high sensitivity and are capable of binding peptides in low nanomolar concentrations (reviewed in van den Pol, 2012). This allows neuropeptide receptors to be activated by very low concentrations of neuropeptides at a greater distance from a release site to provide further support for volume transmission. Similarly to neuropeptides, monoamines that are released extrasynaptically can target glial cells (Zhang et al., 2007; Trueta et al., 2012) in addition to receptors extrasynaptically located on the post-synaptic membrane. In the case of monoamines, dopaminergic D1 receptors in the cerebral cortex are shown to localize in the extrasynaptic space (Smiley et al., 1992; Pérez de la Mora et al., 2008), and in serotonergic neurons, SER-1 and SER-5 receptors are found extrasynaptically (Harris et al., 2011; Jafari et al., 2011). Further supporting extrasynaptic release, projections of serotonergic neurons lacking synaptic specializations can be found in brain areas including the neocortex, striatum, and hippocampus (reviewed in Gianni & Pasqualetti, 2023). The specific mechanism of extrasynaptic release is still not fully understood, and despite evidence of extrasynaptic release existing in neuropeptides and monoamines, extrasynaptic release of glutamate and GABA has not been

observed. This raises the question of why small molecule neurotransmitter release continues to be restricted to active zones rather than also partaking in a form of extrasynaptic release.

Although there has not been any direct evidence of extrasynaptic release, glutamatergic and GABAergic receptors have been identified in the extrasynaptic space. In glutamatergic neurons, AMPA and NMDA receptors are typically located post-synaptically, but some NMDA receptors as well as metabotropic glutamate receptors can be found in the perisynaptic and extrasynaptic plasma membrane (Vizi et al., 2010; Petralia, 2012). Similarly, $GABA_B$ and some $GABA_A$ receptors are found extrasynaptically, such as in granule cells of the cerebellum (Nusser et al., 1998; Vizi et al., 2010). These extrasynaptic receptors often have a high affinity for their respective ligands and thus may be involved in volume transmission. One possible source of neurotransmitter activating extrasynaptic glutamatergic and GABAergic receptors is spill-over from the synaptic cleft (Gladding & Raymond, 2011; Hardingham & Bading, 2010; Trueta et al., 2012). However, the presence of transporters for the reuptake of neurotransmitters and the effective ensheathment of synapses by astroglia may act to minimize spillover in many circumstances (Magi et al., 2019). Another source of neurotransmitter activating extrasynaptic receptors that has been discussed includes neurotransmitter release from glial cells (reviewed in Pál, 2018). The possibility of extrasynaptic release of glutamate and GABA, similar to the extrasynaptic release of neuropeptides and monoamines has so far received little attention. The mechanisms that either confine release to synapses or, as in the case of neuropeptides and monoamines, allow for extrasynaptic release, are likewise not well understood.

Mechanisms Spatially Restricting Release During Synaptic Vesicle Fusion

Based on our current understanding of small molecule neurotransmitter release, the spatial limitation may occur during the fusion stage due to the calcium sensors requirement to be in proximity to VGCCs. From previous literature, it is established that VGCCs concentrate at the active zone (Kaeser et al., 2011; Holderith et al., 2012) thus providing a potential restraint depending on the calcium sensor utilized. In the hippocampus, Syt-1 is expressed as the low-affinity calcium sensor, while Syt-7 and Doc2β act as the high-affinity calcium sensor with nearly a 10-fold and 5-fold greater calcium affinity, respectively (Sugita et al., 2002; Groffen et al, 2006). Due to chelation by calcium-binding proteins and efficient extrusion efforts (Volynski & Krishnakumar, 2018), the required concentration for low-affinity calcium sensor activation can only occur in the calcium nanodomain surrounding the openings of VGCC (Eggermann et al., 2012; Volynski & Krishnakumar, 2018). The spatial restriction of high-affinity calcium sensors has not yet been investigated, but due to their ability to detect trace amounts of calcium, it is reasonable that the asynchronous component of release can occur outside of the confinement of the active zone as trace amounts of calcium diffuse out following an action potential. We hypothesize that the release of small molecule neurotransmitters is restricted to the active zone due to the low-affinity of calcium sensors and the spatially localized calcium transients, but that this spatial restriction can be overcome under circumstances favoring high-affinity calcium sensors to elicit extrasynaptic neurotransmitter release (Hypothesis 1).

Mechanisms Spatially Restricting Release During Synaptic Vesicle Priming

Neurotransmitter release may also be spatially restricted through preferential formation of SNARE complexes at active zones in the priming stage. Most of the proteins that are involved

in synaptic vesicle priming, such as syntaxin and SNAP-25 are found ubiquitously (Hata & Südhof, 1995; Hua & Scheller, 2001a; Vardar et al., 2016; Reddy-Alla et al., 2017). Similarly, Munc-18 lacks confinement to the active zone and is found universally along the axon (Reddy-Alla et al., 2017). However, there is one protein that appears to not be ubiquitous: Munc13 (Brose et al., 1995; Reddy-Alla et al., 2017; Tan et al., 2022a). In mammals, the main isoform of Munc-13, Munc13-1, is mainly found at active zones, presumably due to its interaction with the active zone cytomatrix protein RIM (Betz et al., 2001). Moreover, Munc13-1 not associated with RIM is likely present in an inactive, homodimerized state (Deng et al., 2011). This homodimerization occurs via the C2A domain found in the N-terminus of the protein (Dulubova et al., 2005), and Munc13-1 is only released from this autoinhibition when RIM's Zn-domain binds to Munc13s C2A domain (Dulubova et al., 2005; Deng et al., 2011). This autoinhibition may serve to prevent priming outside the RIM-rich active zone (Deng et al., 2011). Interestingly, the autoinhibition can be overcome by expressing a Munc13 that lacks the C2A domain (Reddy-Alla et al., 2017). A Munc13 version of this nature still retains the MUN-domain and as such can carry out its role in synaptic vesicle priming but will experience a deficit in its localization. At the Drosophila neuromuscular junction, Unc13 lacking the N-terminus but retaining the MUN domain is no longer found confined to the active zone. Instead, it localizes universally throughout the neuromuscular junction similar to syntaxin and Unc18 (Reddy-Alla et al, 2017). Functionally, the expression of a mutant Unc13 with a deleted N-terminus led to additional release sites with low efficiency within the Drosophila neuromuscular junction.

The notion that RIM is required for Munc13-mediated priming is further supported in experiments in which RIM proteins are deleted. With the loss of RIM and ELKS, Munc13 loses

targeting to the active zone, and neurotransmitter release is greatly diminished (Wang et al., 2016; Tan et al., 2022). Active zone localization of Munc13 and release can be fully restored through overexpressing (OE) full-length RIM. Interestingly, overexpressing just the Zn-domain of RIM in a RIM- and ELKS-DKO background is capable of restoring the pool of readily releasable synaptic vesicles and asynchronous release (Tan et al., 2022a), despite causing a mis-localization of Munc13-1 to the "synaptic vesicle cloud" rather than the active zone. This study did not assess whether the neurotransmitter release obtained was changed in its spatial distribution.

When MUNC13 depends on full-length RIM to release it from its homodimerization, it must also be spatial restricted to active zones as RIM also interacts with VGCCs (Kaeser et al., 2011). It may then only be possible for release to occur outside of the active zone in a situation where MUNC13 can be released of its homodimerization independent of full-length RIM as seen in Tan et al. (2022). This unique finding in Tan et al. (2022) leads us to propose the hypothesis that the interaction between RIMs Zn-domain and Munc13-1s C2A-domain that restricts small molecule neurotransmitter release to the active zone, and that this spatial restriction can be overcome in situations lacking this interaction to result in extrasynaptic release (Hypothesis 2).

Assessment of the Spatial Distribution of Synaptic Vesicle Exocytosis

While electrophysiology has the ability to assess synaptic transmission, and by inference neurotransmitter release, with great temporal resolution, it cannot investigate the spatial distribution of release. To investigate how small molecule neurotransmitter release is spatially

restricted to the active zone, we will instead use a cellular imaging approach relying on a fluorescent genetically encoded sensor of synaptic vesicle exocytosis. The hybrid sensors consist of synaptophysin – an integral membrane protein found in synaptic vesicles (Thiel, 1993) – that is tagged with a pH-sensitive GFP fluorescent protein, sypereclipticpHluorin (Miesenböck et al., 1998; Sankaranarayanan et al., 2000) to visualize synaptic vesicles exocytosis. This marker, synaptophysin-pHluorin, is quenched in acidic environments such as the intracellular fluid of synaptic vesicles but fluoresces in neutral environments. As such, when the content of the synaptic vesicle encounters the synaptic cleft, the pH rises and the synaptophysin-pHluorin can fluoresce allowing visualization of exocytosis. When the synaptic vesicle is endocytosed back into the presynaptic neuron the internal environment is re-acidified, and the fluorescence is once again quenched (Figure 1.2). We will additionally express the active zone cytomatrix protein Bassoon with a TdTomato fluorescent protein tag (tdT-Bsn) to mark the location of active zones. Bassoon is precisely restricted to active zones (Dieck et al., 1998; Garner et al., 2000; Mukherjee et al., 2010; Böhme et al., 2016), and as such is an ideal tool for identifying active zones. The use of SypH in junction with tdT-Bsn will allow us to assess the extent of synaptic vesicle exocytosis at the active zone and along the axon outside of the active zone.

Chapter 1 Figures

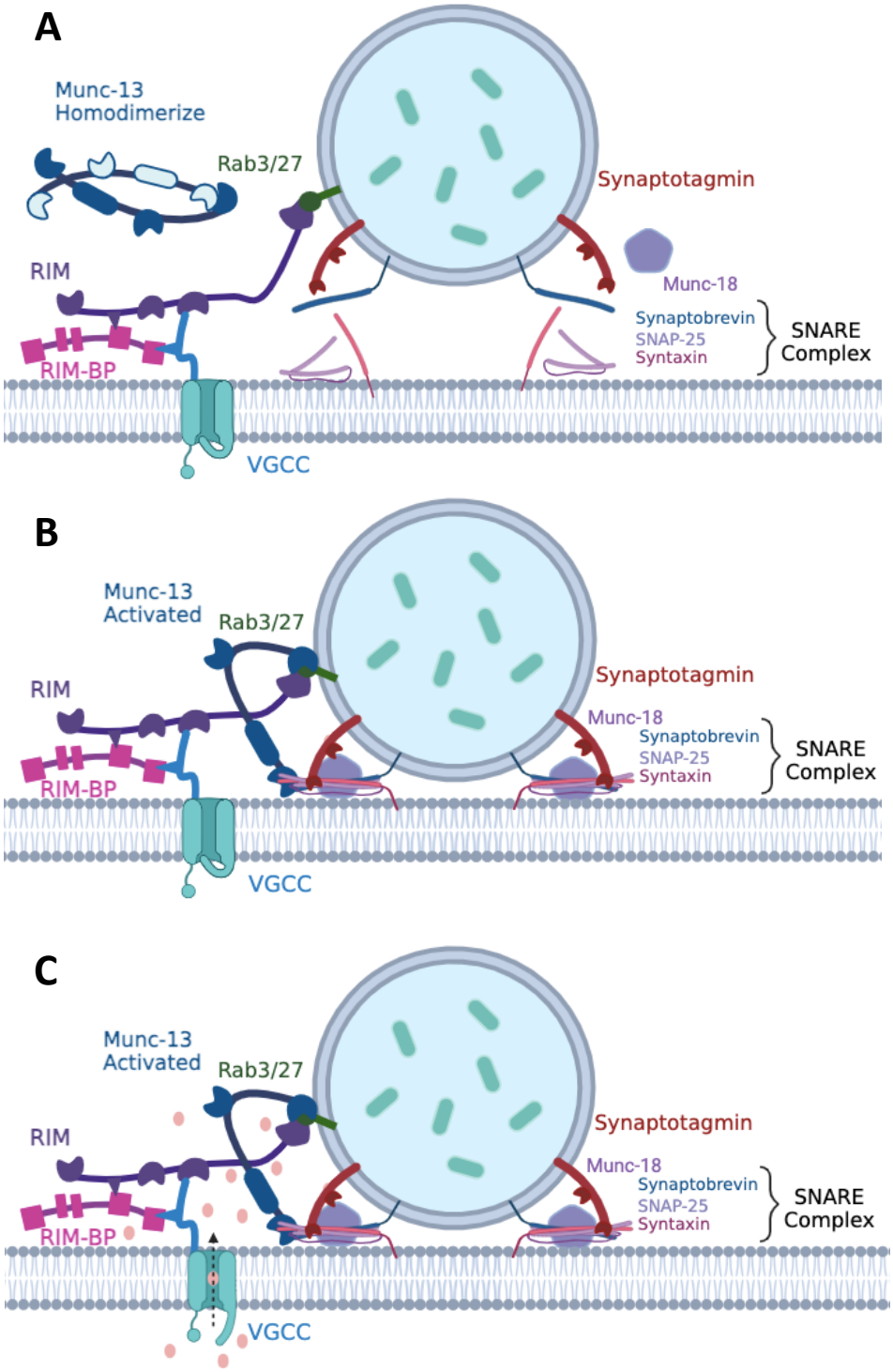

Figure 1.1. Cartoon representation of synaptic vesicle (A) docking, (B) priming, and (C) fusion.

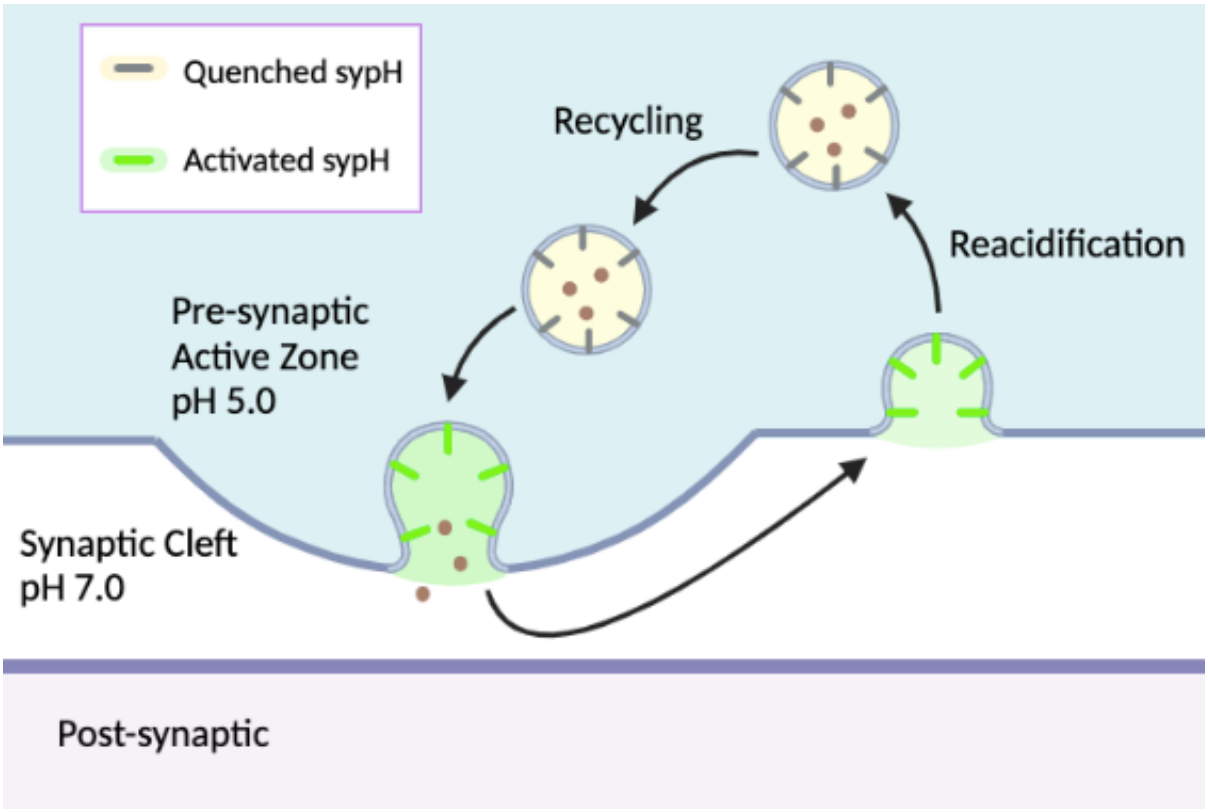

Figure 1.2. Synaptophysin-pHluorin (SypH) is a fluorescent synaptic vesicle-associated protein that is quenched in acidic environments. SypH allows visualization of neurotransmitter release as it encounters the neutral pH of the extracellular environment. Upon endocytosis, SypH fluorescence is quenched by the reacidification of the synaptic vesicle.

CHAPTER 2: METHODS

Hippocampal Cell Cultures

The primary hippocampal neuronal cell cultures were retrieved from mixed-sex E-18 Sprague Dawley rat hippocampi. Approval for euthanasia and dissection of animals was obtained and performed in accordance with the guidelines and regulations outlined by the Dalhousie University Committee on Laboratory Animals (UCLA Protocol #21-108 and #23-072). Neuronal cell culture preparation followed the procedure of Quinn et al. (2019): Hippocampi neurons were incubated in 0.03% trypsin for 15 minutes after dissection to aid in the subsequent mechanical dissociation. Brainphys plating medium, supplemented with SM1 (both from Stemcell Technologies, Vancouver), 0.5mM GlutaMAX, and 5% fetal calf serum (both Thermo Fisher Scientific, Waltham, MA) was used to dilute neurons. At a density of 3-6 x 10^3 cm^{-2}, the neurons were added to 60mm dishes containing five coverslips that were coated with 0.1% poly-L-lysine. After four hours, the plating medium was replaced with serum-free Neurobasal+, supplemented with B-27. Cultures were kept incubated at 5% CO_2 and 37°C and utilized for experiments between 12 and 16 days in vitro.

Expression Constructs

Synaptophysin-pHluorin (SypH)

The hybrid sensor protein synaptophysin-pHluorin (SypH) composed of a pHluorin fused to the vesicle protein synaptophysin was used to visual synaptic vesicle exocytosis (Matz et al., 2010; Quinn et al., 2017). The plasmid used comprises the open reading frame of rat synaptophysin (Genbank accession # NM 012664). Two copies of superecliptic phluorin

(Genbank AY533296), separated and flanked by short flexible linkers were inserted following nucleotide 549 of the synaptophysin ORF. The resulting hybrid protein contains the pHluorin insertion in between transmembrane regions 3 and 4 in its second intraluminal domain.

tdTomato-Bassoon (tdT-Bsn)

The cytomatrix active zone protein Bassoon (Genbank NM 019146) was fluorescently tagged at its N-terminus with tdTomato and co-transfected in hippocampal cultures. Bassoon is restricted to the active zone in both glutamatergic and GABAergic hippocampal synapses (Dieck et al., 1998; Garner et al., 2000). The expression construct employed in this work has been used previously to detect active zone cytomatrices (Matz et al., 2010).

Syt-1 Knockdown Constructs

To knock down synaptotagmin expression we ligated oligonucleotides comprising an inverted palindrome of their respective target sequence, separated by a short hairpin (tctcttgaa or ttcaagaga) into an shRNA expression vector containing a U6 promoter. The mRNA target sequences of the respective shRNA constructs were as follows: sh316 5'-gcagaacatttcacttgaa-3', sh868 5'- atccgatccatacgtcaaa-3', sh1048 5'- gagcaaatccagaaagtgcaa-3', sh1589 5'-ctggctgtcaagaagtaaa-3'. For cellular imaging experiments, SypH, expressed from an EF1alpha promoter) and the respective shRNA, expressed from a U6 promoter, were located on the same plasmid.

Doc2β

The cDNA encoding Doc2β was obtained from Addgene (plasmid #128820). This construct contained a c-terminal EGFP tag, which was removed by PCR to restore the c-

terminus of Doc2β. In cellular imaging experiments, Doc2β and SypH were expressed from the same plasmid utilizing EF1alpha and CMV promoters, respectively.

RIM-ZN

The RIM-ZN construct comprising the first 618 nucleotides of the open reading frame of rat RIM1 (Genbank accession # NM_052829.3) was generated by PCR from a full-length RIM1 construct. The construct differed from the Genbank reference sequence in that it lacked exon 5 (nt 529-540) encoding the amino acids RTKW. For cellular imaging, CMV and EF1alpha promoters, respectively, were used to express RIM-ZN and SypH from the same plasmid.

Munc13-MUN

The Munc13-MUN expression construct is composed of nucleotides 2086-5955 of rat Unc13b (Genbank accession # NM_022862), which encodes the C1, C2B, MUN, and C2C domains that are highly homologous between the Munc13 isoforms. However, the construct lacks the N-terminal half of the protein unique to each Munc13 isoform. To confirm the presence of Munc13-MUN in neurons, the cDNA of mTurquoise was placed at the 3'end of Munc13-MUN, separated by a P2A ribosomal skipping motif. We expressed this deletion mutant under the control of a CMV promoter on a plasmid separate from the plasmid containing the cDNA of SypH, which was co-transfected for imaging experiments. In control neurons, we expressed a plasmid only expressing mTurquoise to allow for blinded experiments.

Calcium Phosphate Transfections

The hippocampal cultures were transfected with a calcium-phosphate precipitation protocol 12-13 days after plating for each experiment. Coverslips were transferred to 60mm

dishes that were prepared with 3mL MEM containing 1:100 B-27 supplement for the transfection. A precipitation mix was made for each dish following the procedure outlined in the Matz et al. (2010) study. The precipitation mix contained 20 µg of plasmid that included the cDNA of tdTomato-Bassoon (tdT-Bsn) and 0.25 M $CaCl_2$ and 80 µg of a plasmid encoding the SypH and water to reach a total volume of 300 µl. For the syt-1 knockdown, Doc2β, and RIM-ZN experiments, shRNAs or cDNAs for RIM-ZN or Doc2β were contained on the plasmid also harboring SypH. For the experiment with the truncated Munc13, we also included x µg of the plasmid encoding Munc13-MUN. Each precipitation mix had 300 µl of HEBS solution (274 mM NaCl, 10 mM KCl, 1.4 mM Na_2HPO_4, 15 mM D- glucose, and 42 mM –(2-hydroxyethlly)-1-piperazineethanesulfonic acid; pH 7.10) slowly added in 100 µl increments and vortexed between each addition. Precipitation mixes were left at room temperature for 20 minutes before mixes were added to respective dishes in a drop-like manner. The dishes containing the transfected neurons were then incubated for 3-4 hours before being washed 3 times in 5-minute intervals with HBS (144 mM NaCl, 3 mM KCl, 2 mM $MgCl_2$, and 10 mM hepes; pH 6.70). Finally, the coverslips were transferred back to their original medium and were incubated at 5% CO_2 and 37°C. Imaging of the neuronal cultures took place 2-5 days after transfection.

Lentivirus transduction

All lentiviruses were produced in HEK293T cells with PEI transfections (Polysciences). HEK293T cells at 60-80% confluency were split 1:4 into 10 cm plates containing 8 mL DMEM the day before transfection. An hour before transfection, the media was removed and replaced with 7.5 mL of transfection medium (DMEM with 2.5% FBS).

DNA mixes were prepared in MEM for each virus containing 1.2 µg pMD2.G, 3 µg psPAX2, and 5.8 µg p.Lenti construct with a total volume of 0.4 mL. A PEI mix containing 500 µl of MEM and 40 µl PEI was then added to each DNA mix for a final volume of 0.8 mL. The mixes were vortexed and then incubated for 20 minutes at room temperature before being added to the cells. After 5 hours 500 µl of growth serum was added to each dish. Lentiviruses were collected 2 days post-transfection and concentrated with Amicon filters with a 10,000 molecular weight cut-off. Each virus was concentrated to about 2 mL.

Neurons were infected with 100 µl of lentivirus 4 days after being cultured and then used for experiments 14 days later.

Immunocytochemistry

Three days after calcium phosphate transfection, neurons were fixed with 4% (v/v) paraformaldehyde and 4% (w/v) sucrose in PBS for 15 minutes at room temperature. Coverslips were washed with PBS three times with five-minute intervals between washes. Then 0.5% triton x-100/PBS was added for 10 minutes then washed again with PBS three times with five-minute intervals between washes. Coverslips were then transferred to parafilm and incubated in blocking solution (1% bovine serum albumin and 0.3% gelatin in PBS) for 1 hour. Mouse monoclonal anti-Syt-1 primary antibody (Millipore) was diluted 1/300 in blocking solution and applied overnight at 4°C. Following the incubation with antibody, the coverslips were washed with PBS for 5 minutes and incubated in blocking solution for 30 minutes. Fluorescein-coupled donkey anti-mouse secondary antibodies (Jackson Immuno) were diluted 1/400 in blocking solution and applied for 1 hour at room temperature. The coverslips were then washed a final

time in PBS before being mounted onto slides using aqua-mount (Thermo Scientific). Slides were then imaged and then analyzed.

Western Blot Validation of Knockdowns

For western blotting, hippocampal neurons were transduced with lentivirus containing either Syt1 sh316 or sh1048 12 days following neuronal plating. 3 days after transduction, neurons were lysed in a RIPA buffer (150mM NaCl,50mM Tris-HCl, 0.5% Sodium Deoxycholate, 10% NP-40). 10 µg of lysed samples per lane were loaded on a 10% SDS-PAGE gel and then transferred to nitrocellulose membranes. Samples were blocked for 1 hour at room temperature with blocking solution (5% non-fat dry milk and 0.1% Tween-20 in TBS) and then incubated with primary antibodies overnight at 4 °C. Membranes were washed three times with 0.1% Tween-20 in TBS, blocked for 30 minutes and then incubated with HRP conjugated secondary antibodies for 1 hour at room temperature. The following antibodies were used: Mouse Anti-synaptotagmin (Chemicon, MAB5202, 1:1000) and Donkey anti-Mouse HRP (Jackson ImmunoResearch, #715-035-150, 1:10’000). HRP signals were detected using a Clarity Max ECL Detection kit (Biorad, Hercules, CA) according to the manufacturer’s instructions, acquired on a ChemiDoc imaging system (BioRad), and analyzed in the FIJI distribution of ImageJ2.

Image Acquisition

All experiments were performed in a HBS solution containing 124 mM NaCl, 3 mM KCl, 2 mM CaCl2, 1 mM MgCl2, 10 mM Hepes, and 5 mM D-glucose (pH 7.30) APV and DNQX were

added to HBS solution at a concentration of 50 µM and 10 µM, respectively, to prevent recurrent excitation. 3 days after calcium phosphate transfection, coverslips were mounted in a stimulation chamber, and immersed in HBS. All images were acquired using a Nikon TE2000 inverted fluorescence microscope equipped with a 60x objective and Hamamatsu ORCA OCCD camera and captured with iVision-Mac software (Biovision Technologies, Exton, PA). Images were acquired at a frequency of 10 Hz. All conditions were blinded to eliminate bias.

Transfected neurons expressing SypH were selected and examined for tdT-Bsn expression. If a transfected neuron with tdT-Bsn expression was found, a test stimulation of 80 stimuli at 80 Hz was applied, as described below, to determine if neurons were responding. If the neurons were sufficiently responding, they were used for an experiment.

Stimulation Procedure

Neurons cultured on coverslips were electrically stimulated with 1 ms square pulses of 10V through two platinum wires spaced 7 mm apart using a SIU-102 stimulus isolator (Warner Instruments, Hamden, CT). Stimulation and acquisition were timed using a Master-8 pulse generator (A.M.P.I., Jerusalem, Israel).

Each field was stimulated with four different paradigms: Isolated stimuli, Bursts of 4 stimuli at 80 Hz, a train of 20 stimuli delivered at 80 Hz, and a train of 80 stimuli at 80 Hz. Each paradigm was repeated at least 40 times for isolated stimuli, 20 times for burst stimuli, and 3 times for each stimulus train. The recovery period between each stimulus paradigm ranged from 5 seconds for isolated stimuli to 2 minutes for longer stimulus trains. Repetitions for the respective stimulation paradigms were averaged together to improve the signal-to-noise ratio of the data.

Analysis

Analysis of the acquired fields was completed with iVision-Mac (Biovision Technologies, Exton, PA). The experimenter remained blinded throughout the analysis.

Analysis of SypH Fluorescence Increases at Synapses and Extrasynaptic Axonal Segments

Images were aligned and background-subtracted. For each experiment, responses were averaged for each stimulation paradigm. Active zones were identified by tdT-Bsn fluorescence and sites with corresponding SypH fluorescence increases were used for analysis. Active zones were excluded if axonal segments were out of focus.

From the point of maximal SypH fluorescence (i.e. the center of the synapse), the change in SypH fluorescence was measured along the axonal segment up to 3 µm where each pixel on the acquired image measures 0.360 µm. We integrated the SypH fluorescence between 0-0.5 µm from the center of the synapse to determine the synaptic response and between 1-3 µm from the center of the synapse to calculate a measure for the perisynaptic response.

Statistical Analysis

For experiments with three conditions, a one-way ANOVA was conducted. Experiments containing two conditions were analyzed with an independent two-sample t-test. Significance was defined by a p-value of less than 0.05.

CHAPTER 3: ROLE OF CALCIUM SENSORS IN THE SPATIAL RESTRICTION OF NEUROTRANSMITTER RELEASE

Effects of Attenuating the Expression of Synaptotagmin-1

As outlined in the introduction, the exocytosis of neurotransmitter may be spatially restricted at the fusion step due to the compartmentalization of calcium signals. In particular, the sensor eliciting synchronous release, Syt-1, exhibits a low affinity for calcium ions and is thought to be activated only in proximity to open VGCCs, which are largely restricted to active zones. Calcium sensors with higher affinity for calcium ions, such as Syt-7, are functional at lower calcium concentrations and may trigger synaptic vesicle fusion at greater distances from sources of calcium influx. However, these high-affinity sensors likely only mediate a smaller fraction of exocytosis, in part because they are suppressed in their function by Syt-1. To assess the spatial extent of synaptic vesicle exocytosis mediated by high-affinity calcium sensors, we expressed shRNA constructs in cultured hippocampal neurons to knock down Syt-1 expression and measure the SypH fluorescence at the active zone, identified by tdT-Bsn, and along the axonal segment. Syt-1 KD efficiency was evaluated with immunocytochemistry and western blot experiments.

Construction and Validation of Knockdown Constructs

We started experimentation with three independent targets within rat Syt-1 mRNA starting at nucleotides 316, 868, and 1589 from the start AUG based on an RNAi target selection algorithm from the Whitehead Institute. Plasmids containing shRNAs complementary to these target sequences or a plasmid devoid of shRNA construct were expressed in neurons together with a plasmid encoding SypH. Three days following transfection, cultures were subjected to immunocytochemistry with an antibody raised against rat Syt-1 used to quantify synaptotagmin

expression. We chose an immunochemistry approach (Figure 3.1) as our transfection method results in maximally 2-5% of neurons expressing proteins or shRNA which makes Western blotting impractical. As demonstrated in Figure 3.1, neurons expressing the sh_316 constructs showed the greatest reduction in Syt-1 immunofluorescence with 47% ± 4% residual Syt-1 expression (n = 15), and as such used it for further experimentation. In contrast, immunofluorescence was reduced to 77% ± 9% in sh_868 expressing neurons (n = 16) and to 62% ± 6% in sh_1589 expressing neurons. A one-way ANOVA revealed a significant difference in Syt-1 immunofluorescence between control and shRNA construct expressing neurons ($F(3,66) = 13.777$, $p < 0.0001$). A post-hoc Tukey test revealed that sh_316 expressing neurons ($p < 0.0001$), sh_868 expressing neurons ($p < 0.05$), and sh_1589 expressing neurons ($p < 0.0001$) were significantly reduced in their Syt-1 immunofluorescence compared to the control neurons.

Despite the significant reduction compared to control neurons, sh_316 transfected neurons exhibited a substantial immunofluorescence which may be either due to a substantial residual Syt-1 expression, non-specific binding of the antibody, or a combination of the two. Due to the possibility of a substantial residual expression, we performed a literature search and selected another shRNA, sh_1048, that has been utilized successfully in a previous study (W. Xu et al., 2012). All further experiments were performed with two shRNA constructs, sh_316 and sh_1048.

To account for the possibility of non-specific antibody binding, we recently further evaluated sh_316 and sh_1048 with a Western blot. Each shRNA construct was inserted into a lentivirus vector and neurons were infected with the produced lentiviruses. In contrast to calcium phosphate transfections, lentivirus increases transfection efficiency substantially, allowing quantification of immunoblotting. Lentivirus-mediated transduction of sh_316 resulted in a

residual expression of Syt-1 of 22.4%, and transduction of sh_1048 resulted in a residual expression of 24.3%. The results of the Western blot (Figure 3.3) require replication and as such the results have not been statistically analyzed.

Effect of Synaptotagmin-1 Knockdown on Synaptic Vesicle Exocytosis

To assess whether Syt-1 contributes to the spatial confinement of neurotransmitter release, we utilized the two shRNA constructs sh_316 and sh_1048. To visualize synaptic vesicle exocytosis, we co-expressed the shRN constructs with SypH which experiences a fluorescence increase when the content of the vesicle encounters the synaptic cleft's neutral pH environment. In addition, we co-expressed tdT-Bsn to visualize the active zone cytomatrix. Neurons expressing either sh_316, sh_1048, or a control plasmid without shRNA were electrically stimulated via extracellular electrodes using four stimulus paradigms: a train of 80 action potentials at 80 Hz, a train of 20 action potentials at 80 Hz, and a short burst of 4 stimuli at 80 Hz, as well as isolated action potentials. Release events mediated by high-affinity calcium sensors will be best revealed in the train of 80 action potentials since this stimulus paradigm sufficiently increases the duration of presynaptic calcium concentrations suited for asynchronous release. In contrast, low-frequency stimulation minimizes asynchronous release as presynaptic calcium transients are brief (Xu et al., 2012). While we are primarily interested in assessing how asynchronous release events affect the spatial extent of synaptic vesicle release, the isolated stimuli are designed to allow us to assess release events mediated by any remaining low-affinity calcium sensors.

Responding synapses exhibiting SypH fluorescence increases that co-localized with tdT-Bsn labeled active zones were selected (Figure 3.2). To assess the spatial distribution of release, the fluorescence increase (ΔF) from the center of the active zone to 3 μm along the axon was

measured for each stimulation condition. Synaptic vesicle exocytosis within 0.5 μm from the center of the active zone was defined as synaptic while exocytosis within 1-3 μm was considered perisynaptic release. Axons from individual neurons containing 8-12 responding active zones were used for analysis affording a total of 9 control axons, 7 sh_316 axons, and 3 sh_1048 axons.

The ΔF in the synaptic area progressively increased with the increasing number of action potentials in the stimulus trains. There was a noticeable ΔF in the perisynaptic area that could be seen following trains of 80 and 20 stimuli, but not following bursts of 4 stimuli (Figure 3.2). The isolated action potential stimulation elicited detectable responses too infrequently that they could be reliably quantified and compared across groups (not shown). Responses in sh_316-transfected neurons, sh_1048-transfected neurons, and neurons transfected with the control plasmid had qualitatively similar ΔF responses (Figure 3.3).

In response to delivering 80 action potentials at 80 Hz (Figure 3.3A), a plot of averaged fluorescence intensities against distance from the active zone center exhibited no obvious difference between groups. During 80 stimuli, the neurons with the control plasmid had an average ΔF of 27.393 (*SE* = 9.131) within the synaptic area and an average ΔF of 10.452 (*SE* = 4.51) in the perisynaptic area. Neurons transfected with sh_316 had an average ΔF of 28.027 (*SE* = 3.734) in the synaptic region and 12.254 (*SE* = 4.692) in the perisynaptic region. Finally, the average ΔF for neurons transfected with sh_1048 was 33.972 (*SE* = 8.134) in the synaptic area and 13.868 (*SE* = 3.334) in the perisynaptic area. A one-way ANOVA revealed no significant difference in ΔF in the synaptic space ($F(2,3) = 1.224$, $p = 0.409$) (Figure 3.3D) Importantly, ΔF in the perisynaptic space was not significantly different between control and Syt-1 KDs (**$F(2,12) = 0.657$, $p = 0.536$) (Figure 3.3E).

In line with the results obtained with 80 stimuli, ΔF in response to 20 stimuli exhibited no appreciable differences between groups when ΔF was plotted against distance from the active zone center (Figure 3.3B), or when synaptic and perisynaptic ΔF were integrated and compared. In the synaptic space, the neurons transfected with the control plasmid had an average ΔF of 12.334 (*SE* = 2.354), and in the perisynaptic space had an average ΔF of 1.888 (*SE* = 1.149). The neurons transfected with sh_316 had an average ΔF of 11.939 (*SE* = 3.151) in the synaptic area and an average ΔF of 3.239 (*SE* = 1.796) in the perisynaptic area. Neurons transfected with sh_1048 had an average ΔF of 14.510 (*SE* = 1.385) in the synaptic area and an average ΔF of 3.471 (*SE* = 1.151) in the perisynaptic area. A one-way ANOVA revealed no significant difference in the synaptic space ($F(2,3) = 0.229$, $p = 0.761$) (Figure 3.3D). Similarly, no significant difference was found in the perisynaptic space ($F(2,12) = 0.981$, $p = 0.403$) (Figure 3.3E).

Finally, ΔF obtained with a short burst of 4 stimuli also elicited very similar fluorescence increases as assessed in the plot of ΔF against distance from the active zone center (Figure 3.3C) and following the integration of synaptic and perisynaptic ΔF. Control neurons had an average ΔF of 5.009 (*SE* = 1.062) in the synaptic area and an average ΔF of 0.325 (*SE* = 0.278) in the perisynaptic area. Neurons transfected with sh_316 showed an average ΔF of 3.847 (*SE* = 0.921) in the synaptic area and an average ΔF of 0.367 (*SE* = 0.262) in the perisynaptic area. Neurons transfected with sh_1048 had an average ΔF of 4.723 (*SE* = 1.277) in the synaptic area and an average ΔF of 0.479 (*SE* = 0.314) in the perisynaptic area. A one-way ANOVA revealed no significant difference in the synaptic space ($F(2,3) = 0.197$, $p = 0.831$) (Figure 3.3D). Similarly, no significant difference was found in the perisynaptic space ($F(2,12) = 0.104$, $p = 0.902$) (Figure 3.3E).

In summary, neurons transfected with Syt-1 KD shRNA constructs did not significantly differ from neurons transfected with a control plasmid in their ΔF within the synaptic or perisynaptic region for any stimulation paradigms.

Doc2β Over-Expression

In a complementary approach to the Syt-1 KD, we sought to assess the effect of overexpressing Doc2β on the spatial restriction of synaptic vesicle exocytosis in neurons. Doc2β is a high-affinity calcium sensor expressed in the hippocampus, but at a considerably reduced rate compared to Syt-isoforms, and consequentially Doc2β-mediated synaptic vesicle exocytosis is also likely limited. However, the extreme sensitivity of Doc2β to calcium ions may allow for release mediated by Doc2β to occur without the spatial restriction to the active zone. To assess whether Doc2β contributes to the spatial confinement of neurotransmitter release, we over-expressed Doc2β with SypH and tdT-Bsn to measure the distribution of exocytosis. Neurons expressing either Doc2β-OE or a control plasmid were stimulated under three conditions: High-frequency trains of 80 and 20 stimuli and bursts of 4 stimuli at 80 Hz. Responding sites with SypH ΔF corresponding to the tdT-Bsn labeled active zones were selected (Figure 3.4). A total of 10 control and 14 Doc2β-overexpressing neurons were used for each stimulation paradigm and analyzed.

In response to trains of 80 stimuli, the plots of ΔF against distance from the center of the active zone were similar (Figure 3.5A) following the integration of the ΔF at synapses and in the perisynaptic area as described above. For neurons transfected with the control plasmid during 80 stimuli, an average ΔF of 20.409 (*SE* = 2.523) was observed in the synaptic area and an average ΔF of 8.102 (*SE* = 1.537) in the perisynaptic area. During the 80 stimuli, neurons over-

expressing Doc2β, with an average ΔF of 20.573 (*SE* = 1.951) in the synaptic area and an average ΔF of 8.050 (*SE* = 1.222) in the perisynaptic area. No significant difference in ΔF was found within the synaptic region, $t(46) = 0.074$, $p = 0.94$, between the and Doc2β-OE (Figure 3.5D). Similarly, the 80 stimulation procedure showed no significant difference in ΔF within the perisynaptic region, $t(118) = 0.063$, $p = 0.95$, between the control and Doc2β-OE (Figure 3.5E).

Responses to 20 stimuli also yielded very similar plots of fluorescence increases against active zone center distance (Figure 3.5B) following the integration of the fluorescence. Neurons transfected with control plasmid during 20 stimuli had an average ΔF of 6.917 (*SE* = 1.407) in the synaptic area, and an average ΔF of 0.660 (*SE* = 0.587) in the perisynaptic area. The neurons with Doc2β-OE had an average ΔF of 6.539 (*SE* = 1.271) in the synaptic area, and an average ΔF of 0.291 (*SE* = 0.519) in the perisynaptic area. There was no significant difference in ΔF found within the synaptic region, $t(46) = 0.281$, $p = 0.78$, between the control and Doc2β-OE (Figure 3.5D). Similarly, the 20 stimulation procedure showed no significant difference in ΔF within the perisynaptic region, $t(118) = 1.041$, $p = 0.30$, between the control and Doc2β-OE (Figure 3.5E).

Finally, fluorescence responses to burst stimulation (4 stimuli) were smaller when plotted against the active zone center distance (Figure 3.5C) following the integration of the fluorescence. Neurons transfected with control plasmid during 4 stimuli had an average ΔF of 3.810 (*SE* = 1.092) in the synaptic area, and an average ΔF of 0.310 (*SE* = 0.377) in the perisynaptic area. The neurons with Doc2β-OE had an average ΔF of 3.525 (*SE* = 0.913) in the synaptic area, and an average ΔF of 0.354 (*SE* = 0.163) in the perisynaptic area. No significant difference in ΔF was found within the synaptic region, $t(46) = 0.281$, $p = 0.78$ (Figure 3.5D), and no significant difference in ΔF within the perisynaptic region, $t(118) = 0.228$, $p = 0.82$, between the control and Doc2β-OE (Figure 3.5E).

In summary, there is no significant difference between neurons transfected with the control plasmid or neurons overexpressing Doc2β in either the synaptic or perisynaptic area for any stimulus paradigm.

Chapter 3 Figures

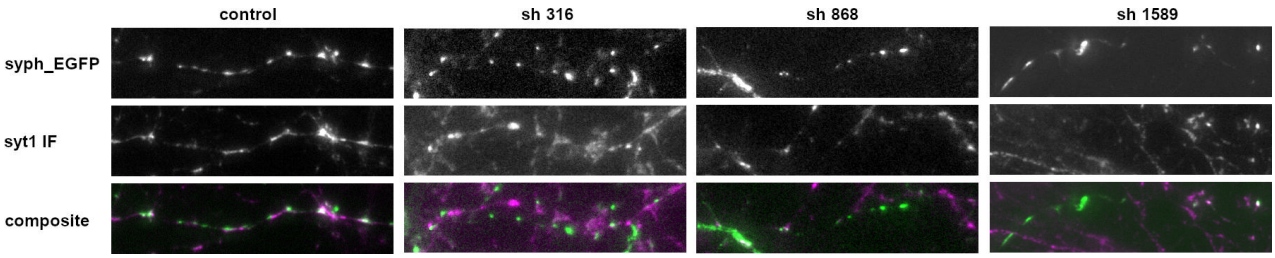

Figure 3.1. Fluorescence microscopy images of neurons stained with SypH_GFP (top row), Syt-1 immunofluorescence (IF) (middle row), and a composite image of SypH_GFP and Syt-1 IF (bottom row) for neurons transfected with a control plasmid, sh_316, sh_868, and sh_1589. Composite images are shown in pseudo coloring with green representing SypH_GFP and purple representing Syt-1 IF.

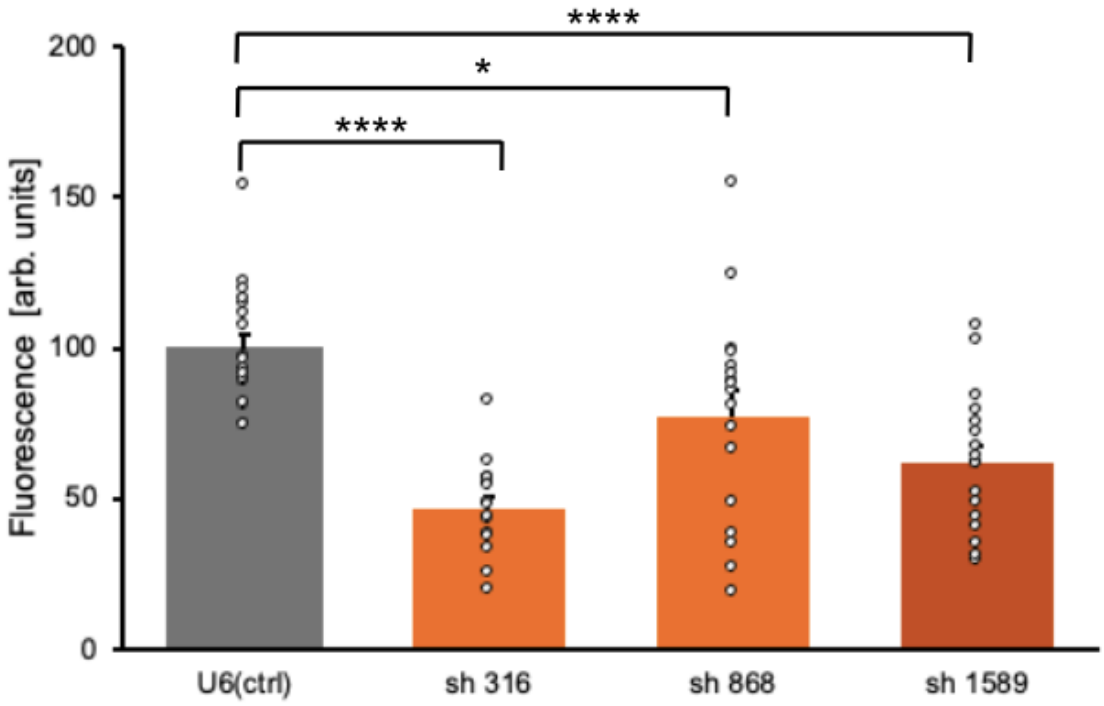

Figure 3.2. Immunocytochemistry showing Syt-1 immunofluorescence in control, sh_316, sh_868, and sh_1589 neurons and biological replicates of each condition

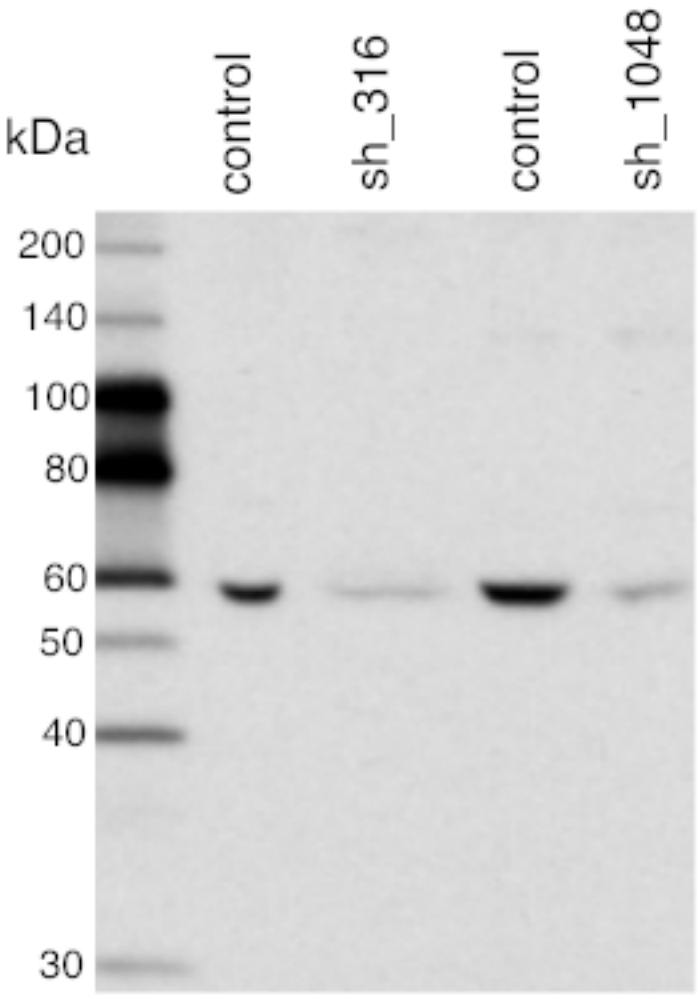

Figure 3.3. Western Blot validation of Syt-1 KD constructs. Lane 1: DNA ladder; Lane 2: control plasmid; Lane 3: sh_316; Lane 4: control plasmid; Lane 5: sh_1048.

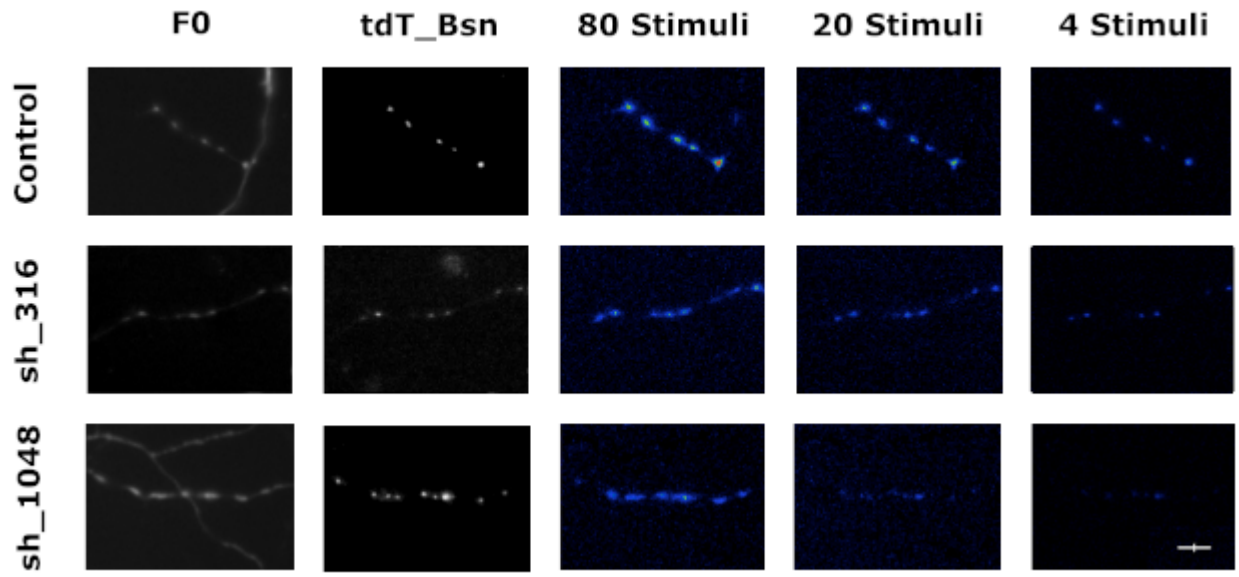

Figure 3.4. Fluorescence microscopy images for Control, sh_316, and sh_1048 showing the SypH fluorescence before stimulation (F0), tdTomato-Bassoon fluorescence (tdT-Bsn) indicating active zones, and SypH fluorescence increases following trains of 80, 20, and 4 stimuli. The SypH fluorescence increase images were obtained by subtracting images taken in the last 300 ms before stimulation from images taken in the 300 ms immediately after stimulation. Fluorescence increases are shown in pseudo coloring where small increases are represented as blue and progressively increase to green, yellow, and finally red. Scale bar: 10 µm.

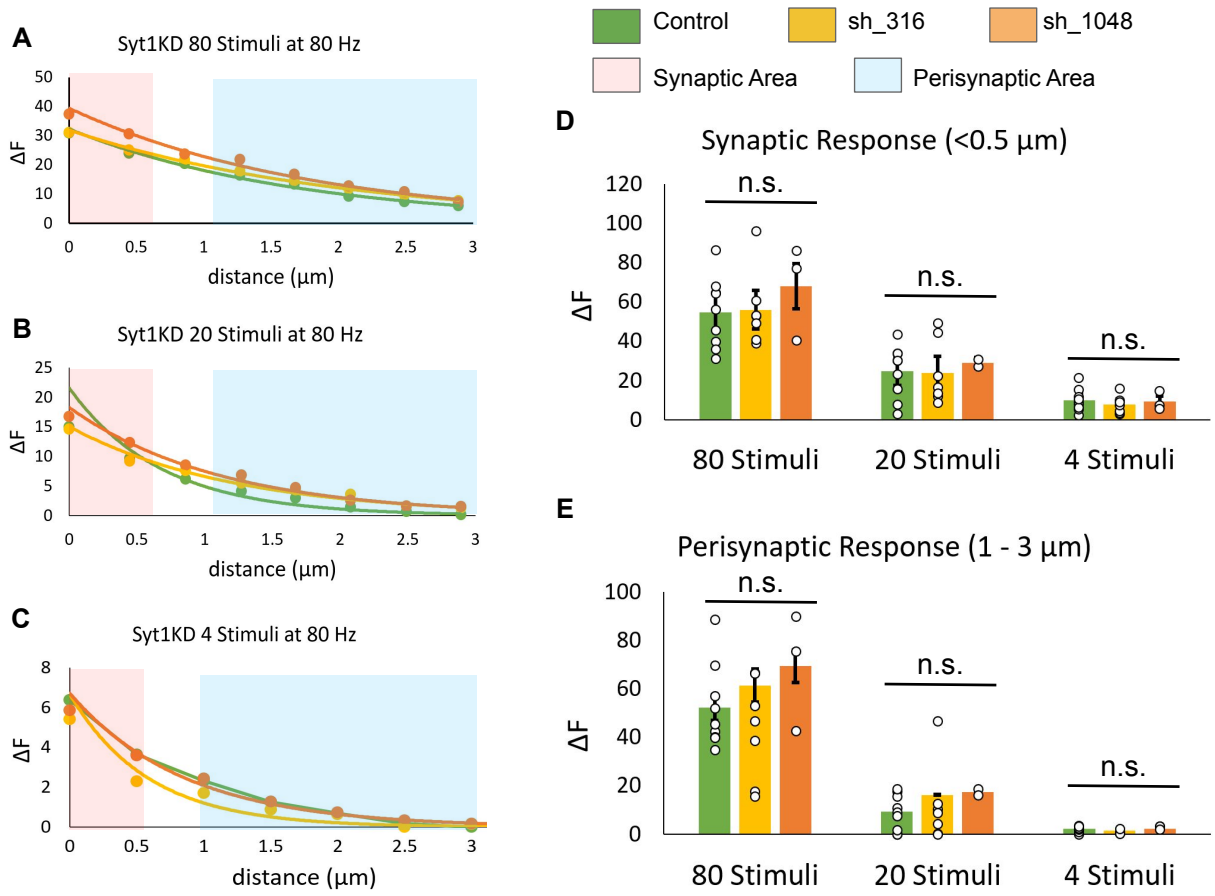

Figure 3.5. (A-C) dF of SypH as a function of distance (µm) for Control, sh_316, and sh_1048 for (A) 80 stimuli, (B) 20 stimuli, and (C) burst of 4 stimuli. Red shaded area represents the synaptic area (<0.5 µm from the center of the bassoon-containing active zone) and the blue shaded area represents the perisynaptic area (1-3 µm). (D) The total fluorescence in the synaptic area (<0.5 µm) for control (n = 9), sh_316 (n = 7), and sh_1048 (n = 3) during 80 stimulation train, 20 stimulation train, and single burst stimulation. (E) The total fluorescence in the perisynaptic area (1-3 µm) for control (n = 9), sh_316 (n = 7), and Sh_1048 (n = 3) during 80 stimulation train, 20 stimulation train, and single burst stimulation.

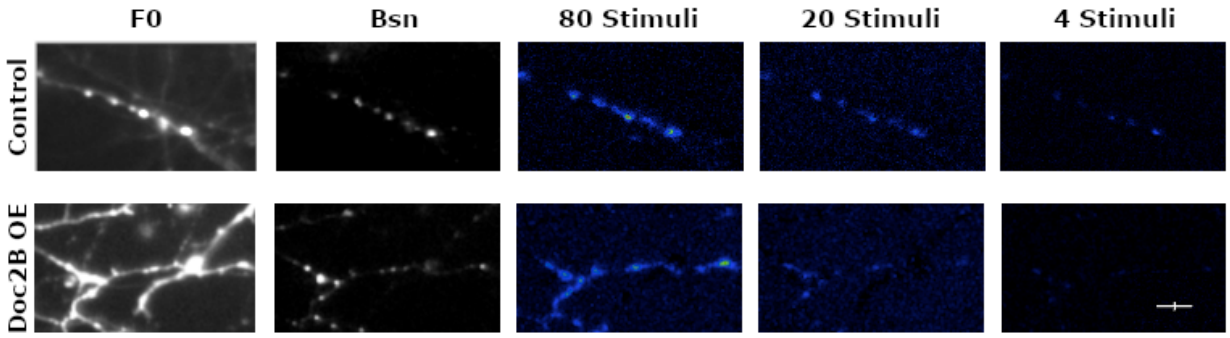

Figure 3.6. Fluorescence microscopy images for Control and Doc2β OE showing the SypH fluorescence before stimulation (F0), tdTomato-Bassoon fluorescence (tdT-Bsn) indicating active zones, and SypH fluorescence increases following trains of 80, 20, and 4 stimuli. The SypH fluorescence increase images were obtained by subtracting images taken in the last 300 ms before stimulation from images taken in the 300 ms immediately after stimulation. Fluorescence increases are shown in pseudo coloring where small increases are represented as blue and progressively increase to green, yellow, and finally red. Scale bar: 10 µm.

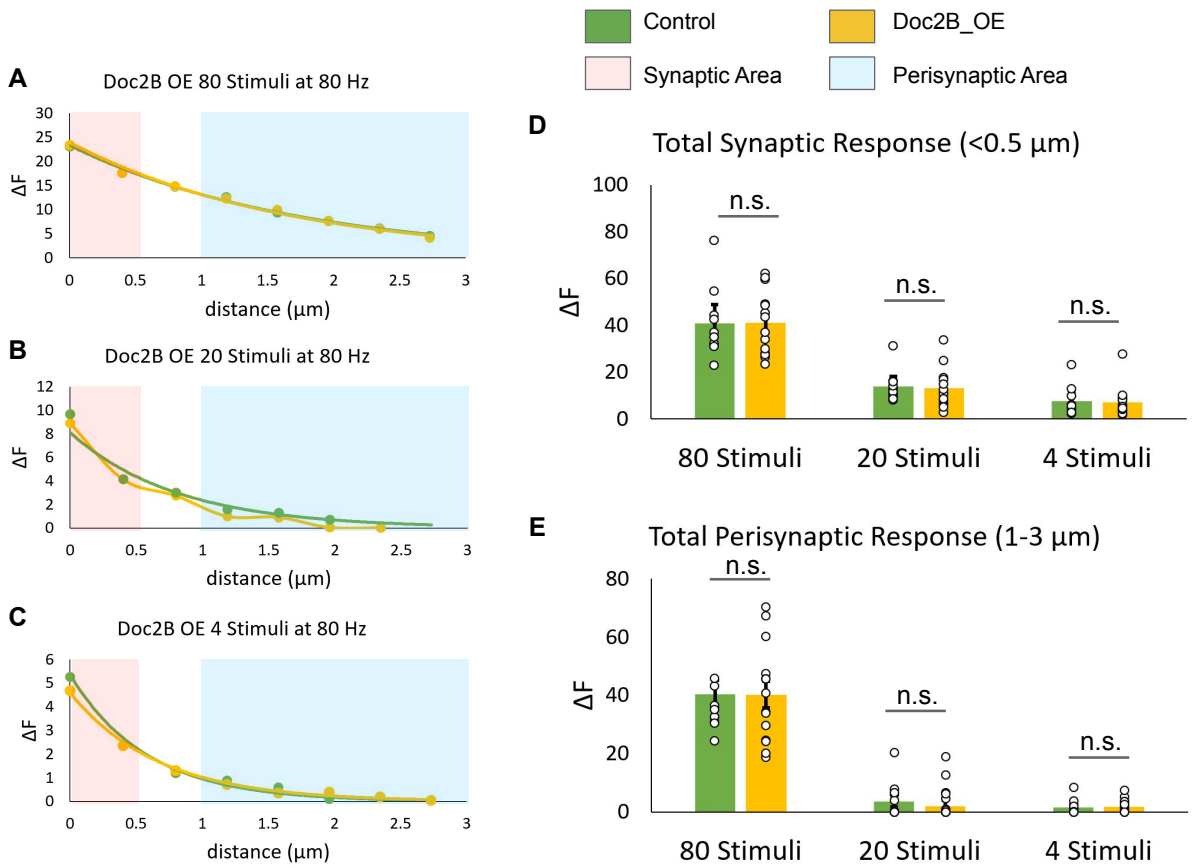

Figure 3.7. (A-C) dF of SypH as a function of distance (µm) for Control and Doc2β_OE for (A) 80 stimuli, (B) 20 stimuli, and (C) burst of 4 stimuli. Red shaded area represents the synaptic area (<0.5 µm from the center of the bassoon-containing active zone) and the blue shaded area represents the perisynaptic area (1-3 µm). (D) The total fluorescence in the synaptic area (<0.5 µm) for control (n = 10) and Doc2β_OE (n = 14) during 80 stimulation train, 20 stimulation train, and single burst stimulation. (E) The total fluorescence in the perisynaptic area (1-3 µm) for control and Doc2β_OE during 80 stimulation train, 20 stimulation train, and single burst stimulation.

CHAPTER 4: ASSESSING THE ROLE OF MUNC13 – RIM INTERACTIONS IN THE SPATIAL RESTRICTION OF SYNAPTIC VESICLE EXOCYTOSIS

Experimental Approaches

The activity of the priming protein Munc13-1 is thought to be largely restricted to the active zone plasma membrane through its interaction with RIM as outlined in the introduction. RIM is stably expressed at the active zone cytomatrix (Kaeser et al., 2011; Nyitrai et al., 2020; Tan et al., 2022), and without RIM's Zn-domain, Munc13-1 cannot be released from its autoinhibition and is unable to catalyze the SNARE complex formation (Dulubova et al., 2005; Deng et al., 2011). This requirement may cause small molecule neurotransmitter release to be spatially restricted to the active zone. This restriction can be overcome experimentally by overexpressing RIM's Zn-finger domain, further abbreviated RIM-ZN. Under these circumstances, the activity of Munc13 is no longer limited to the active zone and may initiate release in the extrasynaptic space (Tan et al., 2022). In a second approach, we will overexpress Munc13's MUN-domain which is constitutively active and capable of engaging in synaptic vesicle priming.

RIM-ZN Over-Expression

To assess whether the interaction between Munc13 and RIM contributes to the spatial confinement of neurotransmitter release, we over-expressed the RIM-ZN domain with SypH and tdT-Bsn to measure the distribution of exocytosis. Neurons expressing either RIM-ZN or a control plasmid were stimulated using three stimulation protocols, either trains of 80 stimuli, 20 stimuli, or bursts of 4 stimuli at 80 Hz. Responding sites with SypH ΔF and corresponding tdT-

Bsn labeled active zones were selected (Figure 4.1). To assess the spatial distribution of release, the ΔF from the center of the active zone to 3 μm along the axon was measured for each stimulation condition. Synaptic vesicle exocytosis within 0.5 μm from the center of the active zone was defined as synaptic while exocytosis within 1-3 μm was considered perisynaptic release. A total of 18 control neurons and 22 RIM-ZN OE neurons were analyzed for each stimulation paradigm.

In response to 80 stimuli at 80 Hz (Figure 4.2A), there was a slight increase in ΔF in neurons overexpressing RIM-Zn compared to neurons transfected with the control plasmid in both the synaptic and perisynaptic area. As seen in the integration of synaptic and perisynaptic fluorescence, control neurons had an average ΔF of 25.193 (*SE* = 2.757) in the synaptic area while the perisynaptic area had an average ΔF of 8.474 (*SE* = 1.504). In comparison, neurons overexpressing RIM-Zn showed an average ΔF of 29.728 (*SE* = 2.985) in the synaptic area and had an average ΔF of 10.398 (*SE* = 1.502) in the perisynaptic area. There was no significant difference in ΔF found within the synaptic region, $t(78) = 1.551$, $p = 0.125$, between the neurons transfected with the control plasmid and neurons overexpressing RIM-ZN OE (Figure 4.2D). However, the 80 stimulation procedure showed a significant difference in ΔF within the perisynaptic region, $t(198) = 2.028$, $p = 0.046$, between the control neurons and RIM-ZN overexpressing neurons (Figure 4.2E).

Following delivery of 20 stimuli at 80 Hz (Figure 4.2B) ΔF was similar in both the synaptic and perisynaptic area between the neurons transfected with the control plasmids and the neurons overexpressing RIM-Zn. Neurons transfected with the control neurons showed an average ΔF of 14.764 (*SE* = 2.362) in the synaptic area and had an average ΔF of 4.406 (*SE* = 1.146) in the perisynaptic space. RIM-Zn overexpressing neurons had an average ΔF of 16.723

(*SE* = 2.522) in the synaptic area and an average ΔF of 4.818 (*SE* = 1.148) in the perisynaptic area. The 20 stimuli had no significant difference in ΔF in the synaptic region, $t(78) = 0.788$, $p = 0.433$ (Figure 4.2D), or in the perisynaptic area, $t(198) = 0.547$, $p = 0.585$, between the control and RIM-ZN OE neurons (Figure 4.2E).

For the burst of 4 stimuli (Figure 4.2C), ΔF was only observed in the synaptic area but was not detectable in the perisynaptic region. The integration of synaptic and perisynaptic fluorescence showed the control neurons with an average ΔF of 2.965 (*SE* = 0.791) in the synaptic area while the RIM-Zn overexpressing neurons had an average ΔF of 3.091 (*SE* = 0.763). The burst of 4 stimuli resulted in no significant difference in ΔF within the synaptic region, $t(46) = 0.124$, $p = 0.902$ (Figure 4.2D), between the control and RIM-ZN OE neurons (Figure 4.2E).

In summary, these results show a significant increase in ΔF between the control neurons and RIM-Zn overexpressing neurons within the perisynaptic area during the train of 80 stimuli. In contrast, there was there is no significant difference between neurons transfected with a control plasmid and neurons overexpressing RIM-Zn under low-frequency trains such as 20 stimuli and 4 stimuli.

Munc13-MUN Over-Expression

To assess whether the interaction between Munc13 and RIM contributes to the spatial confinement of neurotransmitter release, we over-expressed Munc13's MUN domain (M13-MUN OE) with SypH and tdT-Bsn to measure the distribution of exocytosis. Neurons expressing either RIM-ZN or a control plasmid were stimulated under three paradigms: A train of 80 stimuli, a train of 20 stimuli, and a burst of 4 stimuli at 80 Hz. Responding sites with SypH ΔF

corresponding to the tdT-Bsn labeled active zones were selected (Figure 4.3). In a comparison of neurons transfected with the control plasmid (n = 11) and neurons over-expressing Munc13-MUN (n = 13), there was a dramatic increase in ΔF in Munc13-MUN OE neurons in both the synaptic and perisynaptic region during the train of 80 stimuli (Figure 4.4A).

During the train of 80 stimuli (Figure 4.4A), neurons transfected with the control plasmid exhibited an average ΔF of 18.185 (SE = 2.259) in the synaptic area and an average ΔF of 5.406 (SE = 1.003) in the perisynaptic area. Comparatively, neurons over-expressing Munc13-MUN had an average ΔF of 34.002 (SE = 5.027) in the synaptic area and an average ΔF of 11.515 (SE = 2.115) in the perisynaptic area. When ΔF obtained in the synaptic area and in the perisynaptic area were integrated, a significant difference in ΔF was found within the synaptic region, $t(46) = 4.112$, $p = 0.0001$ (Figure 4.4D). Similarly, the 80 stimulation procedure also showed a significant difference in ΔF within the perisynaptic region, $t(94) = 5.591$, $p < 0.0001$, between neurons transfected with the control plasmid and neurons overexpressing Munc13-MUN (Figure 4.4E).

In the train of 20 stimuli (Figure 4.4B), control neurons exhibited an average ΔF of 8.673 (SE = 1.707) in the synaptic area and an average ΔF of 1.880 (SE = 0.723) in the perisynaptic area. Neurons overexpressing Munc13-MUN had an average ΔF of 11.497 (SE = 2.146) in the synaptic region and an average ΔF of 2.215 (SE = 0.587) in the perisynaptic region. The integration of ΔF in the synaptic area and the perisynaptic area revealed no significant difference in ΔF within the synaptic region (Figure 4.4D**)**, $t(46) = 1.421$, $p = 0.162$, or within the perisynaptic region, $t(94) = 0.806$, $p = 0.422$ (Figure 4.4E), between the control neurons and neurons overexpressing Munc13-MUN.

The burst of 4 stimuli (Figure 4.4C) showed neurons transfected with a control plasmid had an average ΔF of 2.619 (*SE* = 0.538) in the synaptic area and an average ΔF of 0.236 (*SE* = 0.143) in the perisynaptic region. In the synaptic area, neurons overexpressing Munc13-MUN had an average ΔF of 2.912 (*SE* = 0.776) while the perisynaptic area had an average ΔF of 0.095 (*SE* = 0.167). There was no significant difference in ΔF was found within the synaptic region, $t(46) = 0.419$, $p = 0.678$ (Figure 4.4D). Similarly, there was no significant difference in ΔF within the perisynaptic region, $t(94) = 1.383$, $p = 0.170$, between the control neurons and neurons overexpressing Munc13-MUN (Figure 4.4E).

In summary, the overexpression of Munc13-MUN resulted in a significant increase in the synaptic and perisynaptic regions during the train of 80 stimuli in comparison to neurons transfected with the control plasmid. Under the train of 20 stimuli and the burst of 4 stimuli, no significant difference was detected between control neurons and those overexpressing Munc13-MUN.

Chapter 4 Figures

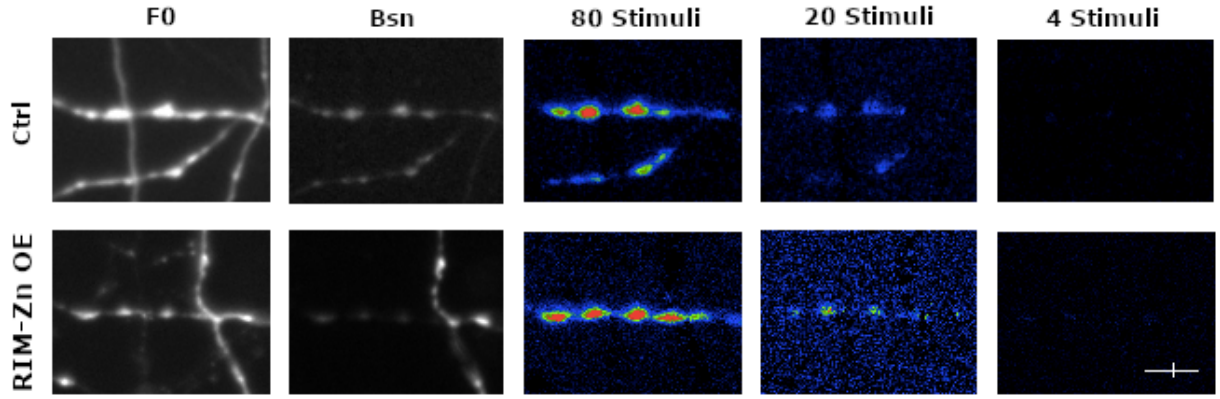

Figure 4.1. Fluorescence microscopy images for Control and RIM-Zn OE showing the SypH fluorescence before stimulation (F0), tdTomato-Bassoon fluorescence (tdT-Bsn) indicating active zones, and SypH fluorescence increases following trains of 80, 20, and 4 stimuli. The SypH fluorescence increase images were obtained by subtracting images taken in the last 300 ms before stimulation from images taken in the 300 ms immediately after stimulation. Fluorescence increases are shown in pseudo coloring where small increases are represented as blue and progressively increase to green, yellow, and finally red. Scale bar: 10 µm.

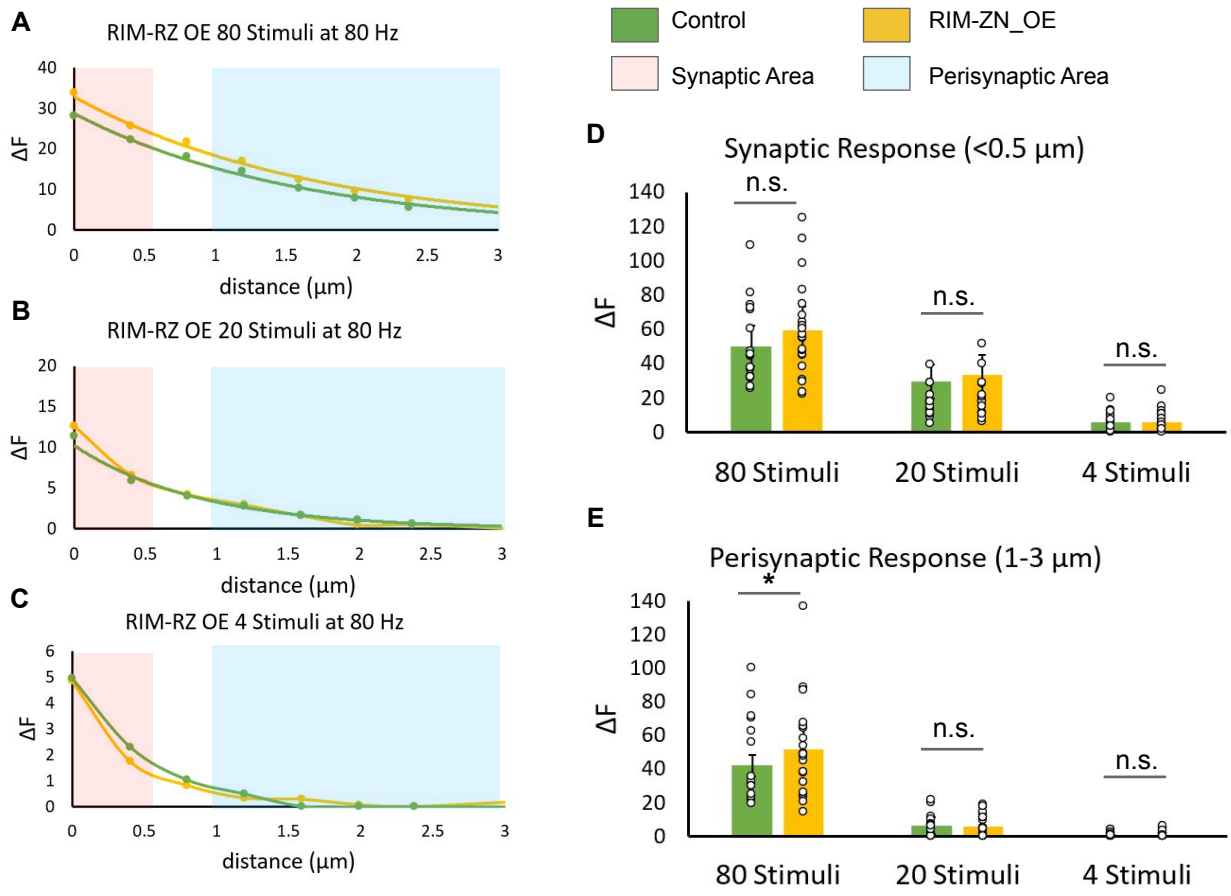

Figure 4.2. (A-C) dF of SypH as a function of distance (μm) for Control and RIM-ZN_OE for (A) 80 stimuli, (B) 20 stimuli, and (C) burst of 4 stimuli. Red shaded area represents the synaptic area (<0.5 μm from the center of the bassoon-containing active zone) and the blue shaded area represents the perisynaptic area (1-3 μm). (D) The total fluorescence in the synaptic area (<0.5 μm) for control (n = 18) and RIM-ZN_OE (n = 22) during 80 stimulation train, 20 stimulation train, and single burst stimulation. (E) The total fluorescence in the perisynaptic area (1-3 μm) for control and RIM-Zn_OE during 80 stimulation train, 20 stimulation train, and single burst stimulation.

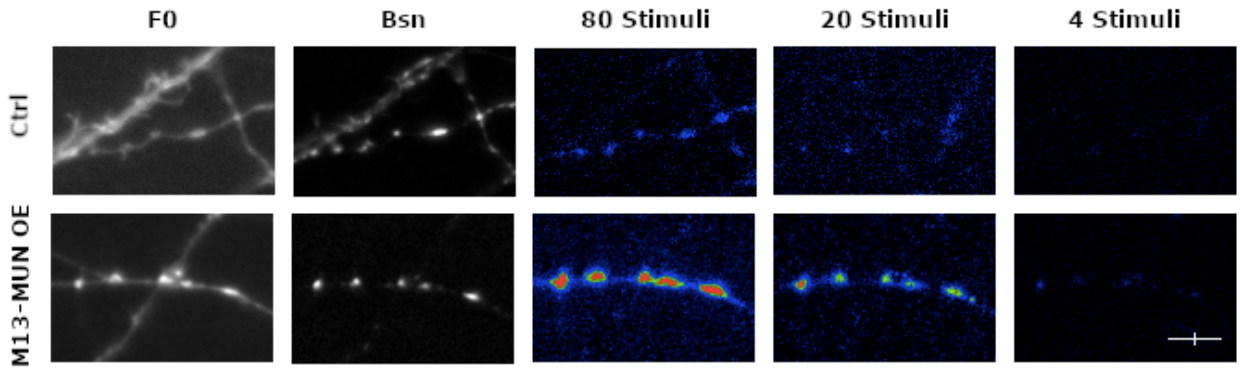

Figure 4.3. Fluorescence microscopy images for Control and Munc13-MUN OE showing the SypH fluorescence before stimulation (F0), tdTomato-Bassoon fluorescence (tdT-Bsn) indicating active zones, and SypH fluorescence increases following trains of 80, 20, and 4 stimuli. The SypH fluorescence increase images were obtained by subtracting images taken in the last 300 ms before stimulation from images taken in the 300 ms immediately after stimulation. Fluorescence increases are shown in pseudo coloring where small increases are represented as blue and progressively increase to green, yellow, and finally red. Scale bar: 10 µm.

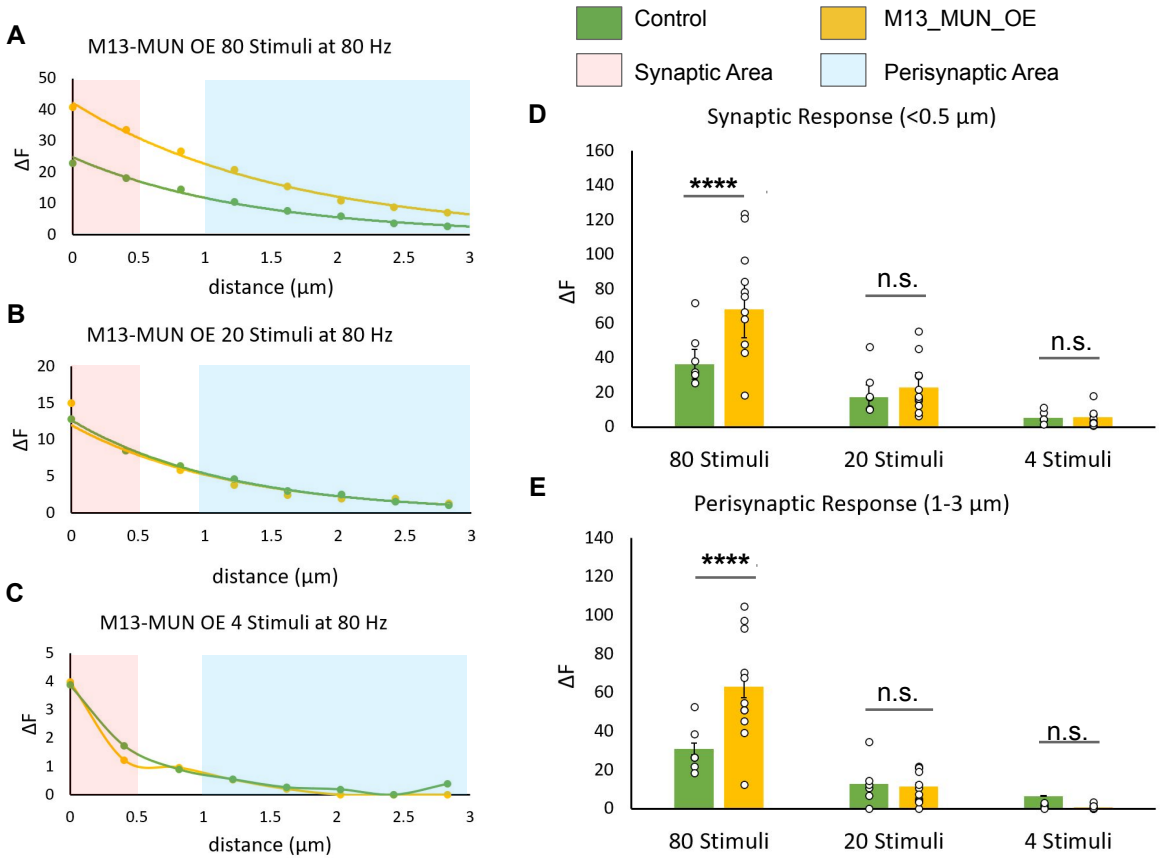

Figure 4.4. (A-C) dF of SypH as a function of distance (µm) for Control and M13-MUN_OE for (A) 80 stimuli, (B) 20 stimuli, and (C) burst of 4 stimuli. Red shaded area represents the synaptic area (<0.5 µm from the center of the bassoon-containing active zone) and the blue shaded area represents the perisynaptic area (1-3 µm). (D) The total fluorescence in the synaptic area (<0.5 µm) for control (n = 11) and M13-MUN_OE (n = 13) during 80 stimulation train, 20 stimulation train, and single burst stimulation. (E) The total fluorescence in the perisynaptic area (1-3 µm) for control and M13-MUN_OE during 80 stimulation train, 20 stimulation train, and single burst stimulation.

CHAPTER 5: DISCUSSION

We set out to elucidate the molecular mechanisms confining small molecule neurotransmitter release to the presynaptic active zone and to investigate if this requirement can be overcome under some circumstances. Convincing evidence exists for the extrasynaptic release of neuropeptides (Trueta & De-Miguel, 2012; Van De Bospoort et al., 2012; Persoon et al., 2019), and monoamines (Zhang et al., 2007; Harris et al., 2011; Jafari et al., 2011; Gianni & Pasqualetti, 2023) acting on extrasynaptic receptors with high ligand affinity in a paracrine fashion (van den Pol, 2012; Gianni & Pasqualetti, 2023). High-affinity glutamate and GABA receptors have also been found in the extrasynaptic plasma membrane (Nusser et al., 1998; Vizi et al., 2010; Petralia, 2012; Magi et al., 2019). However, evidence supporting any extrasynaptic release of glutamate and GABA has not been reported. We have hypothesized that there are two possible mechanisms that could be responsible for restricting small molecule neurotransmitter release to the active zone, a spatial restriction of synaptic vesicle fusion due to the low calcium sensitivity of calcium sensors for synchronous release or the spatial restriction of synaptic vesicle priming through active zone recruitment and regulation of the priming protein Munc-13 by the scaffolding protein RIM.

Calcium Sensors and Their Influence on The Spatial Restriction of Synaptic Vesicle Exocytosis

Calcium influx is detected by calcium-sensing proteins that range in their affinity for calcium. The concentration required for Syt-1 activation, between 10-30 μM, can only be achieved around the opening of VGCCs as calcium is sufficiently chelated following the action potential to control release (Sugita et al., 2002; Volynski & Krishnakumar, 2018). Synaptic

vesicle exocytosis mediated by Syt-1 is likely restricted to the proximity to VGCCs which are located to the active zone (Kaeser et al., 2011; Holderith et al., 2012). However, the hippocampus also expresses the calcium sensors Syt-7 and Doc2B that participate in asynchronous release (Sugita et al., 2001; Bacaj et al., 2013; Kaeser & Regehr, 2014; Turecek & Regehr, 2019). As Syt-7 and Doc2B have a high affinity for calcium ions (Sugita et al., 2002; Groffen et al., 2004; Houy et al., 2017), they might not confer the same spatial limitations to neurotransmitter release as Syt-1 does. Therefore, release events mediated by high-affinity calcium sensors may overcome spatial coupling to the active zone.

Interpretation of Experiments Attenuating Synaptotagmin-1 Expression

To address this hypothesis, we attenuated Syt-1 expression in cultured hippocampal neurons using shRNA constructs to shift release from low-affinity sensor-mediated synchronous release to high-affinity sensor-mediated asynchronous release (DiAntonio & Schwarz, 1994; Geppert et al., 1994; Xu et al., 2007; Bacaj et al., 2013; Chen et al., 2017; Turecek & Regehr, 2019). We expected this KD to limit the synchronous component of neurotransmission while heightening the asynchronous release mediated by high-affinity sensors such as Syt-7. If it is true that high-affinity calcium sensors do not share the spatial requirements as low-affinity calcium sensors, Syt1 KD conditions should show augmented SypH fluorescence increases in what we defined as the perisynaptic space (1-3 μm) compared to control neurons that retain their endogenous Syt-1 expression. The experimental results were unable to support our hypothesis that low-affinity and high-affinity calcium sensors differentially affect the spatial confinement of neurotransmitter release, as we found no significant difference in stimulation-

evoked SypH fluorescence increases within the perisynaptic space (Figure 3.5E) or a shift in the spatial distribution of the fluorescence increases (Figure 3.5).

Of note, we have encountered a technical challenge that limits our ability to refute the hypothesis based on the results of the Syt-1 KD experiment. The residual Syt-1 expression was fairly high with either of the knockdown constructs used (Figure 3.2). It is possible that the remaining Syt-1 expression was capable of allowing substantial synchronous release while sufficiently suppressing the action of sensors such as Syt-7. Our approach to address this possibility was inconclusive. By designing the SypH experiment to include the assessment of exocytosis in response to isolated stimuli, we thought to directly assess Syt-1 mediated release, as release mediated by high-affinity calcium sensors is minimal under these conditions (W. Xu et al., 2012). However, the signal-to-noise ratio of our recordings was not sufficient to reliably compare responses to isolated stimulation. The finding that synaptic fluorescence increases following a burst of 4 stimuli is similar in control and Syt-1 KD neurons is not conclusive, as similar stimulus paradigms already lead to substantial synaptic release mediated by high-affinity sensors (W. Xu et al., 2012). Future experimentation may consider using a Syt-1 knockout mouse to ensure that the Syt-1-mediated release is absent, and any inhibition of high-affinity calcium sensors is eliminated. Alternatively, it may be possible to reduce the residual expression of Syt-1 further by increasing the duration between transfection and time of experimentation. Recently studies have established that Syt-1 has a long turnover with a half-life of about 7 days in culture (Dörrbaum et al., 2018; Vevea & Chapman, 2020). In the present study, we conducted experiments 3 days post-transfection, since neurons have progressively lower viability following calcium phosphate transfections. The duration of knockdown

expression in our experiments may not have provided an adequate amount of time for the neurons to remove endogenous Syt-1. Moreover, it would be valuable to confirm the shift from synchronous to asynchronous release with knockdown expression, for example through patch clamp experiments similar to the ones performed by Xu and collaborators (2012), to conclusively rule out our first hypothesis if long-term knockdown does not lead to a changed spatial profile of neurotransmitter release.

Interpretation of Experiments Overexpressing Doc2β

Our second approach in investigating whether calcium sensors are involved in the spatial restriction of synaptic vesicle exocytosis was to overexpress Doc2β. The calcium affinity of Doc2β is in the submicromolar range, leading to its activation and translocation in the plasma membrane even under conditions of relatively moderate neuronal stimulation (Groffen et al., 2006) and has been implicated in asynchronous release (Yao et al., 2011; Bacaj et al., 2013). Since Doc2β experiences a 10-fold lower expression than that of Syt-isoforms (Bacaj et al., 2013), we reasoned that Doc2β OE could possibly result in an increase in Doc2β-mediated synaptic vesicle exocytosis, allowing us to assess Doc2βs effect on the spatial distribution of release compared to control neurons.

As shown in Figure 3.7, Doc2β OE failed to increase synaptic vesicle exocytosis within the perisynaptic or synaptic space with any of the stimulation paradigms and did not alter the spatial distribution of synaptic vesicle exocytosis (Figure 3.7E), suggesting that heterologously expressed Doc2β is unable to facilitate additional synaptic vesicle exocytosis either at synapses or in the perisynaptic space.

While these findings do not support our hypothesis that low-affinity and high-affinity calcium sensors differentially affect the spatial confinement of neurotransmitter release, they also do not conclusively refute it. We chose to focus our efforts on Doc2β as it is a calcium sensor with particularly high calcium affinity (Groffen et al., 2006) and we hypothesized that as such it would elicit the greatest effect on the spatial distribution of release. However, it is possible that the selection of Doc2B was incorrect. More recently, there has been a debate in the literature as to whether Doc2 proteins play a role in sensing calcium for synaptic vesicle fusion (Díez-Arazola et al., 2020; Khan & Regehr, 2020) or rather as a calcium sensor in the modulation of synaptic vesicle priming (Xue et al., 2018).

Even under the assumption that Doc2 proteins are involved in calcium detection leading to synaptic vesicle fusion, the Doc2β results may be limited by the presence of endogenous Syts. It is well established that Syt-1 clamps the effect of high-affinity calcium sensors such as Syt-7 (Bacaj et al., 2013; Turecek & Regehr, 2019). It is therefore possible that overexpression of high-affinity sensors is ineffective in the presence of Syt-1 due to the ability of the latter sensor to suppress the function of higher-affinity sensors. Future studies may benefit from overexpression of high-affinity calcium sensors on a Syt-1 KO or KD background.

The Influence of Priming on the Spatial Restriction of Synaptic Vesicles Exocytosis

While priming is thought to be confined to the synapse, only Munc13 has been shown to be restricted to the active zone (Brose et al., 1995; Reddy-Alla et al., 2017; Tan et al., 2022) whereas SNARE proteins and Munc18 can be found anywhere in the axon (Hata & Südhof, 1995; Hua & Scheller, 2001; Vardar et al., 2016; Reddy-Alla et al., 2017). We therefore

hypothesized that the interaction of the Munc13-C2A and RIM-Zn domains is responsible for the spatial restriction of Munc13-1 activity in small molecule neurotransmitter release. This interaction between Munc13 and RIM both tethers Munc13 to the active zone plasma membrane (Wang et al., 2016; Tan et al., 2022), and alleviates its autoinhibition (Betz et al., 2001; Dulubova et al., 2005; Tan et al., 2022). Previous studies have shown that this interaction can be bypassed so that Munc13 no longer targets to the presynaptic active zone but can still be released from its homodimer state (Betz et al., 2001; Basu et al., 2005; Wang et al., 2016; Tan et al., 2022), see also Figure 5.1. We undertook two approaches to replicate the interruption of the Munc13-C2A and RIM-Zn interaction resulting in a Munc13 version that is both delocalized and active: RIM-Zn OE or Munc13-MUN OE. If Munc13 is responsible for spatially restricting synaptic vesicle exocytosis, then interrupting this interaction should elicit more release in the perisynaptic space compared to control neurons.

Interpretation of Experiments Overexpressing the RIM-Zn Domain

Our first approach of overexpressing RIM-Zn allows Munc13 to be released from its homodimerized state while not being tethered to the active zone (Wang et al., 2016; Tan et al., 2022) as the PDZ domain of RIM that interacts with VGCCs is removed (Kaeser et al., 2011; Südhof, 2012). RIM OE resulted in significantly larger SypH fluorescence increases in the perisynaptic space compared to control neurons in response to trains of 80 stimuli, but not with trains of 20 or 4 stimuli (Figure 4.2E). Within the synaptic space, we observed no significant difference in SypH fluorescence between the control and RIM-Zn OE with any of the stimulus paradigms, although there was a marginal increase in response to the trains of 80 stimuli (Figure 4.2D). The lack of a significant difference in ΔF with weaker stimulation (trains of 20 or 4

stimuli) in the perisynaptic space may indicate that the effect of Munc13-1 disinhibition by RIM-Zn is only evident in the presence of strongly increased calcium concentrations favoring asynchronous release. Of note, a perturbation of the Munc13-1 and RIM interaction has previously been shown to lead to predominantly asynchronous release (Wang et al., 2016; Kawabe et al., 2017; Nyitrai et al., 2020; Tan et al., 2022), possibly due to the mislocalization of Munc13 away from the active zone, and a subsequent requirement of high-affinity calcium sensors for synaptic vesicle fusion. In summary, these findings appear to support the hypothesis that the Munc13-1 – RIM interaction participates in spatially restricting synaptic vesicle exocytosis to active zones.

Despite the apparent support for the hypothesis, the trend of RIM-Zn OE experiencing increased SypH fluorescence during 80 stimulation in the synaptic space complicates the interpretation of this data. While not significant, the increased synaptic vesicle exocytosis could suggest that the RIM-Zn OE increased total release independent of location. If this is the case, the increased SypH fluorescence in the perisynaptic space may be synaptic-originating and could represent lateral diffusion of SypH out of the synapse into the perisynaptic space, rather than extrasynaptic synaptic vesicle exocytosis.

Interpretation of Experiments Overexpressing Munc13-MUN

Our second approach to addressing whether synaptic vesicle priming spatially restricts the release of small-molecule neurotransmitters was to overexpress the Munc13-MUN construct. This deletion mutant of Munc13 lacks the ability to interact with RIM and is found in a constitutively active state (Betz et al., 2001; Basu et al., 2005). Accordingly, Munc13-MUN OE results in a delocalized, active Munc13 that may be capable of initiating release outside of the

active zone. We observed a significant increase in ΔF in Munc13-MUN overexpressing neurons both at synapses and in the perisynaptic space following trains of 80 stimuli, but not with shorter trains of 20 and 4 stimuli (Figure 4.4). This result, though significant, must be carefully interpreted. As described with the RIM-Zn OE results, it is possible that the increased synaptic vesicle exocytosis at synapses leads to lateral diffusion of exocytosed SypH into the perisynaptic space. Consequently, we cannot at present conclude that release truly occurred in the perisynaptic space and at a greater extent than in the control. Additional experiments will have to be carried out to address our second hypothesis more conclusively.

Future Directions

Munc13-1 KD and the Spatial Control of Neurotransmitter Release

The experiments assessing the role of the RIM – Munc13 interaction in the spatial restriction of release may have yielded inconclusive results because we have overexpressed the Munc13 and RIM deletion constructs on a background of endogenous full-length proteins. As a consequence, the SV exocytosis observed a combination of release mediated by endogenous proteins as well as deletion constructs. In future experiments, it is desirable to attenuate the release mediated by endogenous Munc13 to assess the effects of Munc13 variants lacking the interaction more clearly with RIM. Incidentally, some naturally occurring Munc13 variants lack interactions with RIM. In mammals, Munc13 is transcribed from two genes, Munc13-1 and Munc13-2 (Koch et al., 2000; Betz et al., 2001; Varoqueaux et al., 2002; Böhme et al., 2016; Kawabe et al., 2017; Pooryasin et al., 2021). Furthermore, Munc13-2 has two splice variants (Figure 5.1). The brain-specific Munc13-2 (bMunc13-2) variant is predominant in the mammal

hippocampus and has an N-terminus that lacks the C2A domain interacting with RIM (Varoqueaux et al., 2002; Kawabe et al., 2017). In contrast, the ubiquitous Munc13-2 (ubMunc13-2) variant exhibits a low expression and appears to be redundant to Munc13-1 as it shares a C2A domain-containing N-terminus (Varoqueaux et al., 2002). Instead of interacting with RIM, bMunc13-2 interacts with the docking protein ELKS-1 (Varoqueaux et al., 2002; Kawabe et al., 2017; Nyitrai et al., 2020). While RIM is a cytomatrix active zone protein, ELKS-1 has recently been shown to lack restriction to the active zone and instead associates with the synaptic vesicle cloud (Kawabe et al., 2017; Nyitrai et al., 2020). The localization of bMunc13-2 has not yet been established. Considering that ELKS-1 associates outside of the active zone and that an altered Munc13 can also localize in a similar fashion, it is conceivable that bMunc13-2 also lacks restriction to the active zone. Considering these differences in protein interactions, and possibly location, of Munc13 isoforms, a Munc13-1 KD should be considered to investigate if Munc13-1 is responsible for spatially restricting release and whether its absence elicits a spatial redistribution of release.

Spatial Confinement May Depend on Multiple Mechanisms

The active zone is a highly specialized site that is designed to ensure precise and effective neural communication. It would therefore not be surprising to find that there is not one mechanism alone responsible for the spatial confinement of small molecule neurotransmitter release. Instead, it is very likely that hippocampal neurons are designed to have some redundant systems. Therefore, the spatial confinement of synaptic vesicle exocytosis to the active zone may be controlled by both the low-affinity of Syt-1 and the stable targeting of Munc13-1 to the active zone plasma membrane. It is possible that if synaptic

vesicle exocytosis is capable of occurring perisynaptically in small molecule neurotransmitter release the circumstance requires both a Munc13 protein not tethered to the active zone and a calcium sensor with a high affinity for calcium. Future experiments may consider conducting both a Munc13-1 KD in junction with a Syt-1 KO or KD to ascertain if release mediated by bMunc13-2 and a higher affinity calcium sensor does experience release in the perisynaptic area.

Significance

A better understanding of the sources of GABA and glutamate eliciting the activation of extrasynaptic receptors and volume transmission will aid our understanding of this important non-synaptic form of neuronal communication. The identification of the molecular machinery involved in perisynaptic release will allow us to experimentally manipulate volume transmission to study its role in neuronal input integration and circuit function.

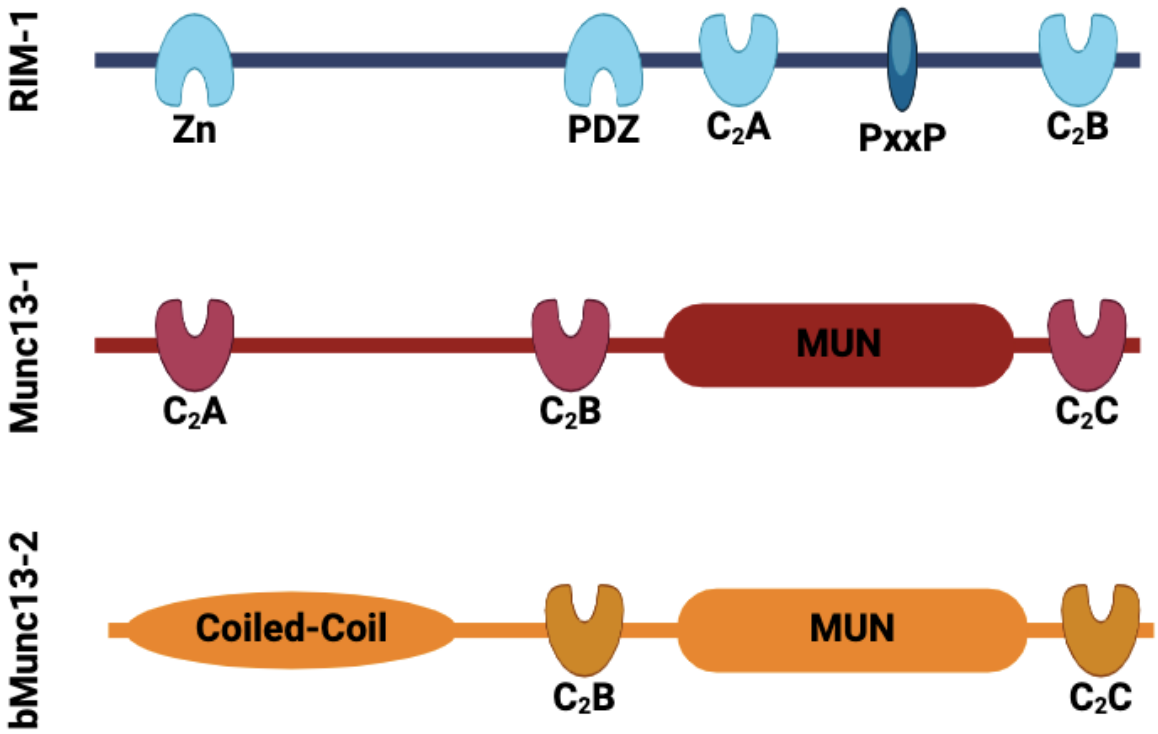

Figure 5.1. Cartoon representation of the proteins RIM-1, Munc13-1, and bMunc13-2.

REFERENCES

Acuna, C., Liu, X., Gonzalez, A., & Südhof, T. C. (2015). RIM-BPs Mediate Tight Coupling of Action Potentials to Ca 2+ -Triggered Neurotransmitter Release. *Neuron*, *87*(6), 1234–1247. https://doi.org/10.1016/j.neuron.2015.08.027

Acuna, C., Liu, X., & Südhof, T. C. (2016). How to Make an Active Zone: Unexpected Universal Functional Redundancy between RIMs and RIM-BPs. *Neuron*, *91*(4), 792–807. https://doi.org/10.1016/j.neuron.2016.07.042

Augustin, I., Rosenmund, C., Südhof, T. C., & Brose, N. (1999). Munc13-1 is essential for fusion competence of glutamatergic synaptic vesicles. *Nature*, *400*(6743), 457–461. https://doi.org/10.1038/22768

Bacaj, T., Wu, D., Yang, X., Morishita, W., Zhou, P., Xu, W., Malenka, R. C., & Südhof, T. C. (2013). Synaptotagmin-1 and Synaptotagmin-7 Trigger Synchronous and Asynchronous Phases of Neurotransmitter Release. *Neuron*, *80*(4), 947–959. https://doi.org/10.1016/j.neuron.2013.10.026

Basu, J., Shen, N., Dulubova, I., Lu, J., Guan, R., Guryev, O., Grishin, N. V., Rosenmund, C., & Rizo, J. (2005). A minimal domain responsible for Munc13 activity. *Nature Structural & Molecular Biology*, *12*(11), 1017–1018. https://doi.org/10.1038/nsmb1001

Betz, A., Thakur, P., Junge, H. J., Ashery, U., Rhee, J.-S., Scheuss, V., Rosenmund, C., Rettig, J., & Brose, N. (2001). Functional Interaction of the Active Zone Proteins Munc13-1 and RIM1 in Synaptic Vesicle Priming. *Neuron*, *30*(1), 183–196. https://doi.org/10.1016/S0896-6273(01)00272-0

Blasi, J., Chapman, E. R., Link, E., Binz, T., Yamasaki, S., Camilli, P. D., Südhof, T. C., Niemann, H., & Jahn, R. (1993). Botulinum neurotoxin A selectively cleaves the synaptic protein SNAP-25. *Nature*, *365*(6442), 160–163. https://doi.org/10.1038/365160a0

Blasi, J., Chapman, E. R., Yamasaki, S., Binz, T., Niemann, H., & Jahn, R. (1993). Botulinum neurotoxin C1 blocks neurotransmitter release by means of cleaving HPC-1/syntaxin. *The EMBO Journal*, *12*(12), 4821–4828. https://doi.org/10.1002/j.1460-2075.1993.tb06171.x

Böhme, M. A., Beis, C., Reddy-Alla, S., Reynolds, E., Mampell, M. M., Grasskamp, A. T., Lützkendorf, J., Bergeron, D. D., Driller, J. H., Babikir, H., Göttfert, F., Robinson, I. M., O'Kane, C. J., Hell, S. W., Wahl, M. C., Stelzl, U., Loll, B., Walter, A. M., & Sigrist, S. J. (2016). Active zone scaffolds differentially accumulate Unc13 isoforms to tune Ca2+ channel–vesicle coupling. *Nature Neuroscience*, *19*(10), 1311–1320. https://doi.org/10.1038/nn.4364

Brose, N., Hofmann, K., Hata, Y., & Südhof, T. C. (1995). Mammalian Homologues of Caenorhabditis elegans unc-13 Gene Define Novel Family of C2-domain Proteins. *Journal of Biological Chemistry*, *270*(42), 25273–25280. https://doi.org/10.1074/jbc.270.42.25273

Bunin, M. A., & Wightman, R. M. (1998). Quantitative Evaluation of 5-Hydroxytryptamine (Serotonin) Neuronal Release and Uptake: An Investigation of Extrasynaptic Transmission. *The Journal of Neuroscience*, *18*(13), 4854–4860. https://doi.org/10.1523/JNEUROSCI.18-13-04854.1998

Chang, S., Trimbuch, T., & Rosenmund, C. (2018). Synaptotagmin-1 drives synchronous Ca2+-triggered fusion by C2B-domain-mediated synaptic-vesicle-membrane attachment. *Nature Neuroscience*, *21*(1), 33–40. https://doi.org/10.1038/s41593-017-0037-5

Chapman, E. R., An, S., Edwardson, J. M., & Jahn, R. (1996). A Novel Function for the Second C2 Domain of Synaptotagmin. *Journal of Biological Chemistry*, *271*(10), 5844–5849. https://doi.org/10.1074/jbc.271.10.5844

Chen, C., Arai, I., Satterfield, R., Young, S. M., & Jonas, P. (2017). Synaptotagmin 2 Is the Fast Ca2+ Sensor at a Central Inhibitory Synapse. *Cell Reports*, *18*(3), 723–736. https://doi.org/10.1016/j.celrep.2016.12.067

Deken, S. L. (2005). Redundant Localization Mechanisms of RIM and ELKS in Caenorhabditis elegans. *Journal of Neuroscience*, *25*(25), 5975–5983. https://doi.org/10.1523/JNEUROSCI.0804-05.2005

De-Miguel, F. F., Leon-Pinzon, C., Torres-Platas, S. G., del-Pozo, V., Hernández-Mendoza, G. A., Aguirre-Olivas, D., Méndez, B., Moore, S., Sánchez-Sugía, C., García-Aguilera, M. A., Martínez-Valencia, A., Ramírez-Santiago, G., & Rubí, J. M. (2021). Extrasynaptic Communication. *Frontiers in Molecular Neuroscience*, *14*, 638858. https://doi.org/10.3389/fnmol.2021.638858

Deng, L., Kaeser, P. S., Xu, W., & Südhof, T. C. (2011). RIM Proteins Activate Vesicle Priming by Reversing Autoinhibitory Homodimerization of Munc13. *Neuron*, *69*(2), 317–331. https://doi.org/10.1016/j.neuron.2011.01.005

DiAntonio, A., & Schwarz, T. L. (1994). The Effect on Synaptic Physiology of synaptotagmin Mutations in Drosophila. *Neuron*, *12*(April), 909–920.

Diao, J., Su, Z., Lu, X., Yoon, T.-Y., Shin, Y.-K., & Ha, T. (2010). Single-Vesicle Fusion Assay Reveals Munc18-1 Binding to the SNARE Core Is Sufficient for Stimulating Membrane Fusion. *ACS Chemical Neuroscience*, *1*(3), 168–174. https://doi.org/10.1021/cn900034p

Dieck, S., Sanmartí-Vila, L., Langnaese, K., Richter, K., Kindler, S., Soyke, A., Wex, H., Smalla, K.-H., Kämpf, U., Fränzer, J.-T., Stumm, M., Garner, C. C., & Gundelfinger, E. D. (1998). Bassoon, a Novel Zinc-finger CAG/Glutamine-repeat Protein Selectively Localized at the Active Zone of Presynaptic Nerve Terminals. *Journal of Cell Biology*, *142*(2), 499–509. https://doi.org/10.1083/jcb.142.2.499

Díez-Arazola, R., Meijer, M., Bourgeois-Jaarsma, Q., Cornelisse, L. N., Verhage, M., & Groffen, A. J. (2020). Doc2 Proteins Are Not Required for the Increased Spontaneous Release Rate in Synaptotagmin-1-Deficient Neurons. *The Journal of Neuroscience*, *40*(13), 2606–2617. https://doi.org/10.1523/JNEUROSCI.0309-19.2020

Dörrbaum, A. R., Kochen, L., Langer, J. D., & Schuman, E. M. (2018). Local and global influences on protein turnover in neurons and glia. *eLife*, *7*, e34202. https://doi.org/10.7554/eLife.34202

Dulubova, I., Lou, X., Lu, J., Huryeva, I., Alam, A., Schneggenburger, R., Südhof, T. C., & Rizo, J. (2005). A Munc13/RIM/Rab3 tripartite complex: From priming to plasticity? *The EMBO Journal*, *24*(16), 2839–2850. https://doi.org/10.1038/sj.emboj.7600753

Eggermann, E., Bucurenciu, I., Goswami, S. P., & Jonas, P. (2012). Nanodomain coupling between Ca2+ channels and sensors of exocytosis at fast mammalian synapses. *Nature Reviews Neuroscience*, *13*(1), 7–21. https://doi.org/10.1038/nrn3125

Friedrich, R., Groffen, A. J., Connell, E., Van Weering, J. R. T., Gutman, O., Henis, Y. I., Davletov, B., & Ashery, U. (2008). DOC2B Acts as a Calcium Switch and Enhances Vesicle Fusion. *Journal of Neuroscience*, *28*(27), 6794–6806. https://doi.org/10.1523/JNEUROSCI.0538-08.2008

Fuxe, K., Borroto-Escuela, D. O., Romero-Fernandez, W., Ciruela, F., Manger, P., Leo, G., Díaz-Cabiale, Z., & Agnati, L. F. (2012). On the role of volume transmission and receptor–receptor interactions in social behaviour: Focus on central catecholamine and oxytocin neurons. *Brain Research*, *1476*, 119–131. https://doi.org/10.1016/j.brainres.2012.01.062

Garner, C. C., Kindler, S., & Gundelfinger, E. D. (2000). Molecular determinants of presynaptic active zones. *Current Opinion in Neurobiology*, *10*(3), 321–327. https://doi.org/10.1016/S0959-4388(00)00093-3

Geppert, M., Goda, Y., Hammer, R. E., Li, C., Rosahl, T. W., Stevens, C. F., & Südhof, T. C. (1994). Synaptotagmin I: A major Ca2+ sensor for transmitter release at a central synapse. *Cell*, *79*(4), 717–727. https://doi.org/10.1016/0092-8674(94)90556-8

Gerber, S. H., Rah, J.-C., Min, S.-W., Liu, X., de Wit, H., Dulubova, I., Meyer, A. C., Rizo, J., Arancillo, M., Hammer, R. E., Verhage, M., Rosenmund, C., & Südhof, T. C. (2008). Conformational Switch of Syntaxin-1 Controls Synaptic Vesicle Fusion. *Science*, *321*(5895), 1507–1510. https://doi.org/10.1126/science.1163174

Gianni, G., & Pasqualetti, M. (2023). Wiring and Volume Transmission: An Overview of the Dual Modality for Serotonin Neurotransmission. *ACS Chemical Neuroscience*, *14*(23), 4093–4104. https://doi.org/10.1021/acschemneuro.3c00648

Gladding, C. M., & Raymond, L. A. (2011). Mechanisms underlying NMDA receptor synaptic/extrasynaptic distribution and function. *Molecular and Cellular Neuroscience*, *48*(4), 308–320. https://doi.org/10.1016/j.mcn.2011.05.001

Groffen, A., Friedrich, R., Brian, E. C., Ashery, U., & Verhage, M. (2006). DOC2A and DOC2B are sensors for neuronal activity with unique calcium-dependent and kinetic properties: DOC2A and DOC2B are sensors for neuronal activity. *Journal of Neurochemistry*, *97*(3), 818–833. https://doi.org/10.1111/j.1471-4159.2006.03755.x

Groffen, A. J. A., Brian, E. C., Dudok, J. J., Kampmeijer, J., Toonen, R. F., & Verhage, M. (2004). Ca2+-induced Recruitment of the Secretory Vesicle Protein DOC2B to the Target Membrane. *Journal of Biological Chemistry*, *279*(22), 23740–23747. https://doi.org/10.1074/jbc.M400731200

Groffen, A. J., Martens, S., Arazola, R. D., Cornelisse, L. N., Lozovaya, N., de Jong, A. P. H., Goriounova, N. A., Habets, R. L. P., Takai, Y., Borst, J. G., Brose, N., McMahon, H. T., & Verhage, M. (2010). Doc2b Is a High-Affinity Ca $^{2+}$ Sensor for Spontaneous Neurotransmitter Release. *Science*, *327*(5973), 1614–1618. https://doi.org/10.1126/science.1183765

Hallermann, S., Fejtova, A., Schmidt, H., Weyhersmüller, A., Silver, R. A., Gundelfinger, E. D., & Eilers, J. (2010). Bassoon Speeds Vesicle Reloading at a Central Excitatory Synapse. *Neuron*, *68*(4), 710–723. https://doi.org/10.1016/j.neuron.2010.10.026

Han, G. A., Bin, N.-R., Kang, S.-Y. A., Han, L., & Sugita, S. (2013). The domain-3a of Munc18-1 plays a crucial role at the priming stage of exocytosis. *Journal of Cell Science*, jcs.126862. https://doi.org/10.1242/jcs.126862

Hardingham, G. E., & Bading, H. (2010). Synaptic versus extrasynaptic NMDA receptor signalling: Implications for neurodegenerative disorders. *Nature Reviews Neuroscience*, *11*(10), 682–696. https://doi.org/10.1038/nrn2911

Harris, G., Korchnak, A., Summers, P., Hapiak, V., Law, W. J., Stein, A. M., Komuniecki, P., & Komuniecki, R. (2011). Dissecting the Serotonergic Food Signal Stimulating Sensory-Mediated Aversive Behavior in C. elegans. *PLoS ONE*, *6*(7), e21897. https://doi.org/10.1371/journal.pone.0021897

Hata, Y., & Südhof, T. C. (1995). A Novel Ubiquitous Form of Munc-18 Interacts with Multiple Syntaxins. *Journal of Biological Chemistry*, *270*(22), 13022–13028. https://doi.org/10.1074/jbc.270.22.13022

Held, R. G., & Kaeser, P. S. (2018). ELKS active zone proteins as multitasking scaffolds for secretion. *Open Biology*, *8*(2), 170258. https://doi.org/10.1098/rsob.170258

Held, R. G., Liu, C., & Kaeser, P. S. (2016). ELKS controls the pool of readily releasable vesicles at excitatory synapses through its N-terminal coiled-coil domains. *eLife*, *5*, e14862. https://doi.org/10.7554/eLife.14862

Hibino, H., Pironkova, R., Onwumere, O., Vologodskaia, M., Hudspeth, A. J., & Lesage, F. (2002). RIM Binding Proteins (RBPs) Couple Rab3-Interacting Molecules (RIMs) to Voltage-Gated Ca2+ Channels. *Neuron*, *34*(3), 411–423. https://doi.org/10.1016/S0896-6273(02)00667-0

Holderith, N., Lorincz, A., Katona, G., Rózsa, B., Kulik, A., Watanabe, M., & Nusser, Z. (2012). Release probability of hippocampal glutamatergic terminals scales with the size of the active zone. *Nature Neuroscience*, *15*(7), 988–997. https://doi.org/10.1038/nn.3137

Houy, S., Groffen, A. J., Ziomkiewicz, I., Verhage, M., Pinheiro, P. S., & Sørensen, J. B. (2017). Doc2B acts as a calcium sensor for vesicle priming requiring synaptotagmin-1, Munc13-2 and SNAREs. *eLife*, *6*, e27000. https://doi.org/10.7554/eLife.27000

Hua, Y., & Scheller, R. H. (2001a). Three SNARE complexes cooperate to mediate membrane fusion. *Proceedings of the National Academy of Sciences*, *98*(14), 8065–8070. https://doi.org/10.1073/pnas.131214798

Hua, Y., & Scheller, R. H. (2001b). Three SNARE complexes cooperate to mediate membrane fusion. *Proceedings of the National Academy of Sciences*, *98*(14), 8065–8070. https://doi.org/10.1073/pnas.131214798

Jafari, G., Xie, Y., Kullyev, A., Liang, B., & Sze, J. Y. (2011). Regulation of Extrasynaptic 5-HT by Serotonin Reuptake Transporter Function in 5-HT-Absorbing Neurons Underscores Adaptation Behavior in Caenorhabditis elegans. *Journal of Neuroscience*, *31*(24), 8948–8957. https://doi.org/10.1523/JNEUROSCI.1692-11.2011

Kaeser, P. S., Deng, L., Wang, Y., Dulubova, I., Liu, X., Rizo, J., & Südhof, T. C. (2011). RIM Proteins Tether Ca2+ Channels to Presynaptic Active Zones via a Direct PDZ-Domain Interaction. *Cell*, *144*(2), 282–295. https://doi.org/10.1016/j.cell.2010.12.029

Kaeser, P. S., & Regehr, W. G. (2014). Molecular Mechanisms for Synchronous, Asynchronous, and Spontaneous Neurotransmitter Release. *Annual Review of Physiology*, *76*(1), 333–363. https://doi.org/10.1146/annurev-physiol-021113-170338

Kasai, H., Takahashi, N., & Tokumaru, H. (2012). Distinct Initial SNARE Configurations Underlying the Diversity of Exocytosis. *Physiological Reviews*, *92*(4), 1915–1964. https://doi.org/10.1152/physrev.00007.2012

Kawabe, H., Mitkovski, M., Kaeser, P. S., Hirrlinger, J., Opazo, F., Nestvogel, D., Kalla, S., Fejtova, A., Verrier, S. E., Bungers, S. R., Cooper, B. H., Varoqueaux, F., Wang, Y., Nehring, R. B., Gundelfinger, E. D., Rosenmund, C., Rizzoli, S. O., Südhof, T. C., Rhee, J.-S., & Brose, N. (2017). ELKS1 localizes the synaptic vesicle priming protein bMunc13-2 to a specific subset of active zones. *Journal of Cell Biology*, *216*(4), 1143–1161. https://doi.org/10.1083/jcb.201606086

Khan, M. M., & Regehr, W. G. (2020). Loss of Doc2b does not influence transmission at Purkinje cell to deep nuclei synapses under physiological conditions. *eLife*, *9*, e55165. https://doi.org/10.7554/eLife.55165

Koch, H., Hofmann, K., & Brose, N. (2000). *Definition of Munc13-homology-domains and characterization of a novel ubiquitously expressed Munc13 isoform*. 7.

Liu, C., Bickford, L. S., Held, R. G., Nyitrai, H., Sudhof, T. C., & Kaeser, P. S. (2014). The Active Zone Protein Family ELKS Supports Ca2+ Influx at Nerve Terminals of Inhibitory Hippocampal Neurons. *Journal of Neuroscience*, *34*(37), 12289–12303. https://doi.org/10.1523/JNEUROSCI.0999-14.2014

Mackler, J. M., Drummond, J. A., Loewen, C. A., Robinson, I. M., & Reist, N. E. (2002). The C2B Ca2+-binding motif of synaptotagmin is required for synaptic transmission in vivo. *Nature*, *418*(6895), 340–344. https://doi.org/10.1038/nature00846

Magi, S., Piccirillo, S., Amoroso, S., & Lariccia, V. (2019). Excitatory Amino Acid Transporters (EAATs): Glutamate Transport and Beyond. *International Journal of Molecular Sciences*, *20*(22), 5674. https://doi.org/10.3390/ijms20225674

Martin, S., Tomatis, V. M., Papadopulos, A., Christie, M. P., Malintan, N. T., Gormal, R. S., Sugita, S., Martin, J. L., Collins, B. M., & Meunier, F. A. (2013). The Munc18-1 domain 3a loop is essential for neuroexocytosis but not for syntaxin-1A transport to the plasma membrane. *Journal of Cell Science*, *126*(11), 2353–2360. https://doi.org/10.1242/jcs.126813

Matz, J., Gilyan, A., Kolar, A., McCarvill, T., & Krueger, S. R. (2010). Rapid structural alterations of the active zone lead to sustained changes in neurotransmitter release. *Proceedings of the National Academy of Sciences*, *107*(19), 8836–8841. https://doi.org/10.1073/pnas.0906087107

Miesenböck, G., De Angelis, D. A., & Rothman, J. E. (1998). Visualizing secretion and synaptic transmission with pH-sensitive green fluorescent proteins. *Nature*, *394*(6689), 192–195. https://doi.org/10.1038/28190

Mochida, S., Orita, S., Sakaguchi, G., Sasaki, T., & Takai, Y. (1998). Role of the Doc2␣–Munc13–1 interaction in the neurotransmitter release process. *Proc. Natl. Acad. Sci. USA*.

Mukherjee, K., Yang, X., Gerber, S. H., Kwon, H.-B., Ho, A., Castillo, P. E., Liu, X., & Südhof, T. C. (2010). Piccolo and bassoon maintain synaptic vesicle clustering without directly participating in vesicle exocytosis. *Proceedings of the National Academy of Sciences*, *107*(14), 6504–6509. https://doi.org/10.1073/pnas.1002307107

Nusser, Z., Sieghart, W., & Somogyi, P. (1998). Segregation of Different GABA $_A$ Receptors to Synaptic and Extrasynaptic Membranes of Cerebellar Granule Cells. *The Journal of Neuroscience*, *18*(5), 1693–1703. https://doi.org/10.1523/JNEUROSCI.18-05-01693.1998

Nyitrai, H., Wang, S. S. H., & Kaeser, P. S. (2020). ELKS1 Captures Rab6-Marked Vesicular Cargo in Presynaptic Nerve Terminals. *Cell Reports*, *31*(10), 107712. https://doi.org/10.1016/j.celrep.2020.107712

Ohtsuka, T., Takao-Rikitsu, E., Inoue, E., Inoue, M., Takeuchi, M., Matsubara, K., Deguchi-Tawarada, M., Satoh, K., Morimoto, K., Nakanishi, H., & Takai, Y. (2002). CAST: a novel protein of the cytomatrix at the active zone of synapses that forms a ternary complex with RIM1 and Munc13-1. *The Journal of Cell Biology*, *158*(3), 577–590. https://doi.org/10.1083/jcb.200202083

Orita, S., Naito, A., Sakaguchi, G., Maeda, M., Igarashi, H., Sasaki, T., & Takai, Y. (1997). Physical and Functional Interactions of Doc2 and Munc13 in Ca2+-dependent Exocytotic Machinery. *Journal of Biological Chemistry*, *272*(26), 16081–16084. https://doi.org/10.1074/jbc.272.26.16081

Pál, B. (2018). Involvement of extrasynaptic glutamate in physiological and pathophysiological changes of neuronal excitability. *Cellular and Molecular Life Sciences*, *75*(16), 2917–2949. https://doi.org/10.1007/s00018-018-2837-5

Pang, Z. P., Bacaj, T., Yang, X., Zhou, P., Xu, W., & Südhof, T. C. (2011). Doc2 Supports Spontaneous Synaptic Transmission by a Ca2+-Independent Mechanism. *Neuron*, *70*(2), 244–251. https://doi.org/10.1016/j.neuron.2011.03.011

Persoon, C. M., Hoogstraaten, R. I., Nassal, J. P., Van Weering, J. R. T., Kaeser, P. S., Toonen, R. F., & Verhage, M. (2019). The RAB3-RIM Pathway Is Essential for the Release of Neuromodulators. *Neuron*, *104*(6), 1065-1080.e12. https://doi.org/10.1016/j.neuron.2019.09.015

Petralia, R. S. (2012). Distribution of Extrasynaptic NMDA Receptors on Neurons. *The Scientific World Journal*, *2012*, 1–11. https://doi.org/10.1100/2012/267120

Pevsner, J., Hsu, S.-C., Braun, J. E. A., Calakos, N., Ting, A. E., Bennett, M. K., & Scheller, R. H. (1994). Specificity and regulation of a synaptic vesicle docking complex. *Neuron*, *13*(2), 353–361. https://doi.org/10.1016/0896-6273(94)90352-2

Pinheiro, P. S., Houy, S., & Sørensen, J. B. (2016). C2-domain containing calcium sensors in neuroendocrine secretion. *Journal of Neurochemistry*, *139*(6), 943–958. https://doi.org/10.1111/jnc.13865

Pooryasin, A., Maglione, M., Schubert, M., Matkovic-Rachid, T., Hasheminasab, S., Pech, U., Fiala, A., Mielke, T., & Sigrist, S. J. (2021). Unc13A and Unc13B contribute to the decoding of distinct sensory information in Drosophila. *Nature Communications*, *12*(1), 1932. https://doi.org/10.1038/s41467-021-22180-6

Quinn, D. P., Kolar, A., Wigerius, M., Gomm-Kolisko, R. N., Atwi, H., Fawcett, J. P., & Krueger, S. R. (2017). Pan-neurexin perturbation results in compromised synapse stability and a reduction in readily releasable synaptic vesicle pool size. *Scientific Reports*, *7*(1), 42920. https://doi.org/10.1038/srep42920

Reddy-Alla, S., Böhme, M. A., Reynolds, E., Beis, C., Grasskamp, A. T., Mampell, M. M., Maglione, M., Jusyte, M., Rey, U., Babikir, H., McCarthy, A. W., Quentin, C., Matkovic, T., Bergeron, D. D., Mushtaq, Z., Göttfert, F., Owald, D., Mielke, T., Hell, S. W., … Walter, A. M. (2017). Stable Positioning of Unc13 Restricts Synaptic Vesicle Fusion to Defined Release Sites to Promote Synchronous Neurotransmission. *Neuron*, *95*(6), 1350-1364.e12. https://doi.org/10.1016/j.neuron.2017.08.016

Richmond, J. E., Weimer, R. M., & Jorgensen, E. M. (2001). An open form of syntaxin bypasses the requirement for UNC-13 in vesicle priming. *Nature*, *412*(6844), 338–341. https://doi.org/10.1038/35085583

Rizo, J., & Xu, J. (2015). The Synaptic Vesicle Release Machinery. *Annual Review of Biophysics*, *44*(1), 339–367. https://doi.org/10.1146/annurev-biophys-060414-034057

Sankaranarayanan, S., De Angelis, D., Rothman, J. E., & Ryan, T. A. (2000). The Use of pHluorins for Optical Measurements of Presynaptic Activity. *Biophysical Journal*, *79*(4), 2199–2208. https://doi.org/10.1016/S0006-3495(00)76468-X

Schiavo, G. G., Benfenati, F., Poulain, B., Rossetto, O., De Laureto, P. P., DasGupta, B. R., & Montecucco, C. (1992). Tetanus and botulinum-B neurotoxins block neurotransmitter release by proteolytic cleavage of synaptobrevin. *Nature*, *359*(6398), 832–835. https://doi.org/10.1038/359832a0

Schoch, S., Deák, F., Königstorfer, A., Mozhayeva, M., Sara, Y., Südhof, T. C., & Kavalali, E. T. (2001). SNARE Function Analyzed in Synaptobrevin/VAMP Knockout Mice. *Science*, *294*(5544), 1117–1122. https://doi.org/10.1126/science.1064335

Stevens, C. F., & Sullivan, J. M. (2003). The Synaptotagmin C2A Domain Is Part of the Calcium Sensor Controlling Fast Synaptic Transmission. *Neuron*, *39*(2), 299–308. https://doi.org/10.1016/S0896-6273(03)00432-X

Stevens, D. R., Wu, Z.-X., Matti, U., Junge, H. J., Schirra, C., Becherer, U., Wojcik, S. M., Brose, N., & Rettig, J. (2005). Identification of the Minimal Protein Domain Required for Priming Activity of Munc13-1. *Current Biology*, *15*(24), 2243–2248. https://doi.org/10.1016/j.cub.2005.10.055

Südhof, T. C. (2012). The Presynaptic Active Zone. *Neuron*, *75*(1), 11–25. https://doi.org/10.1016/j.neuron.2012.06.012

Sugita, S., Han, W., Butz, S., Liu, X., Fernández-Chacón, R., Lao, Y., & Südhof, T. C. (2001). Synaptotagmin VII as a Plasma Membrane Ca2+ Sensor in Exocytosis. *Neuron*, *30*(2), 459–473. https://doi.org/10.1016/S0896-6273(01)00290-2

Sugita, S., Shin, O.-H., Han, W., & Lao, Y. (2002). *Synaptotagmins form a hierarchy of exocytotic Ca2+ sensors with distinct Ca2+ af®nities*. 11.

Tan, C., Wang, S. S. H., de Nola, G., & Kaeser, P. S. (2022a). Rebuilding essential active zone functions within a synapse. *Neuron*, *110*(9), 1498-1515.e8. https://doi.org/10.1016/j.neuron.2022.01.026

Tan, C., Wang, S. S. H., de Nola, G., & Kaeser, P. S. (2022b). Rebuilding essential active zone functions within a synapse. *Neuron*, *110*(9), 1498-1515.e8. https://doi.org/10.1016/j.neuron.2022.01.026

Thiel, G. (1993). Synapsin I, Synapsin II, and Synaptophysin: Marker Proteins of Synaptic Vesicles. *Brain Pathology*, *3*(1), 87–95. https://doi.org/10.1111/j.1750-3639.1993.tb00729.x

Toonen, R. F. G., De Vries, K. J., Zalm, R., Südhof, T. C., & Verhage, M. (2005). Munc18–1 stabilizes syntaxin 1, but is not essential for syntaxin 1 targeting and SNARE complex formation. *Journal of Neurochemistry*, *93*(6), 1393–1400. https://doi.org/10.1111/j.1471-4159.2005.03128.x

Trueta, C., & De-Miguel, F. F. (2012). Extrasynaptic exocytosis and its mechanisms: A source of molecules mediating volume transmission in the nervous system. *Frontiers in Physiology*, *3*. https://doi.org/10.3389/fphys.2012.00319

Trueta, C., Kuffler, D. P., & De-Miguel, F. F. (2012). Cycling of Dense Core Vesicles Involved in Somatic Exocytosis of Serotonin by Leech Neurons. *Frontiers in Physiology*, *3*. https://doi.org/10.3389/fphys.2012.00175

Turecek, J., & Regehr, W. G. (2019). Neuronal Regulation of Fast Synaptotagmin Isoforms Controls the Relative Contributions of Synchronous and Asynchronous Release. *Neuron*, *101*(5), 938-949.e4. https://doi.org/10.1016/j.neuron.2019.01.013

Van De Bospoort, R., Farina, M., Schmitz, S. K., De Jong, A., De Wit, H., Verhage, M., & Toonen, R. F. (2012). Munc13 controls the location and efficiency of dense-core vesicle release in neurons. *Journal of Cell Biology*, *199*(6), 883–891. https://doi.org/10.1083/jcb.201208024

van den Pol, A. N. (2012). Neuropeptide Transmission in Brain Circuits. *Neuron*, *76*(1), 98–115. https://doi.org/10.1016/j.neuron.2012.09.014

Vardar, G., Chang, S., Arancillo, M., Wu, Y.-J., Trimbuch, T., & Rosenmund, C. (2016). Distinct Functions of Syntaxin-1 in Neuronal Maintenance, Synaptic Vesicle Docking, and Fusion in Mouse Neurons. *The Journal of Neuroscience*, *36*(30), 7911–7924. https://doi.org/10.1523/JNEUROSCI.1314-16.2016

Varoqueaux, F., Sigler, A., Rhee, J.-S., Brose, N., Enk, C., Reim, K., & Rosenmund, C. (2002). Total arrest of spontaneous and evoked synaptic transmission but normal synaptogenesis in the absence of Munc13-mediated vesicle priming. *Proceedings of the National Academy of Sciences*, *99*(13), 9037–9042. https://doi.org/10.1073/pnas.122623799

Verhage, M., Maia, A. S., Plomp, J. J., Brussaard, A. B., Heeroma, J. H., Vermeer, H., Toonen, R. F., Hammer, R. E., Van Den, T. K., Berg, Missler, M., Geuze, H. J., & Südhof, T. C. (2000). Synaptic Assembly of the Brain in the Absence of Neurotransmitter Secretion. *Science*, *287*(5454), 864–869. https://doi.org/10.1126/science.287.5454.864

Vevea, J. D., & Chapman, E. R. (2020). Acute disruption of the synaptic vesicle membrane protein synaptotagmin 1 using knockoff in mouse hippocampal neurons. *eLife*, *9*, e56469. https://doi.org/10.7554/eLife.56469

Vizi, E., Fekete, A., Karoly, R., & Mike, A. (2010). Non-synaptic receptors and transporters involved in brain functions and targets of drug treatment: Non-synaptic receptors involved in brain functions. *British Journal of Pharmacology*, *160*(4), 785–809. https://doi.org/10.1111/j.1476-5381.2009.00624.x

Volynski, K. E., & Krishnakumar, S. S. (2018). Synergistic control of neurotransmitter release by different members of the synaptotagmin family. *Current Opinion in Neurobiology*, *51*, 154–162. https://doi.org/10.1016/j.conb.2018.05.006

Wang, S. S. H., Held, R. G., Wong, M. Y., Liu, C., Karakhanyan, A., & Kaeser, P. S. (2016). Fusion Competent Synaptic Vesicles Persist upon Active Zone Disruption and Loss of Vesicle Docking. *Neuron*, *91*(4), 777–791. https://doi.org/10.1016/j.neuron.2016.07.005

Wang, Y., Okamoto, M., Schmitz, F., Hofmann, K., & Südhof, T. C. (1997). Rim is a putative Rab3 effector in regulating synaptic-vesicle fusion. *Nature*, *388*(6642), 593–598. https://doi.org/10.1038/41580

Wang, Y., Sugita, S., & Südhof, T. C. (2000). The RIM/NIM Family of Neuronal C2 Domain Proteins. *Journal of Biological Chemistry*, *275*(26), 20033–20044. https://doi.org/10.1074/jbc.M909008199

Weimer, R. M., Richmond, J. E., Davis, W. S., Hadwiger, G., Nonet, M. L., & Jorgensen, E. M. (2003). Defects in synaptic vesicle docking in unc-18 mutants. *Nature Neuroscience*, *6*(10), 1023–1030. https://doi.org/10.1038/nn1118

Xu, J., Mashimo, T., & Südhof, T. C. (2007). Synaptotagmin-1, -2, and -9: Ca2+ Sensors for Fast Release that Specify Distinct Presynaptic Properties in Subsets of Neurons. *Neuron*, *54*(4), 567–581. https://doi.org/10.1016/j.neuron.2007.05.004

Xu, W., Morishita, W., Buckmaster, P. S., Pang, Z. P., Malenka, R. C., & Südhof, T. C. (2012). Distinct Neuronal Coding Schemes in Memory Revealed by Selective Erasure of Fast Synchronous Synaptic Transmission. *Neuron*, *73*(5), 990–1001. https://doi.org/10.1016/j.neuron.2011.12.036

Xu, Y., Su, L., & Rizo, J. (2010). Binding of Munc18-1 to Synaptobrevin and to the SNARE Four-Helix Bundle. *Biochemistry*, *49*(8), 1568–1576. https://doi.org/10.1021/bi9021878

Xue, R., Ruhl, D. A., Briguglio, J. S., Figueroa, A. G., Pearce, R. A., & Chapman, E. R. (2018). Doc2-mediated superpriming supports synaptic augmentation. *Proceedings of the National Academy of Sciences*, *115*(24). https://doi.org/10.1073/pnas.1802104115

Yang, X., Wang, S., Sheng, Y., Zhang, M., Zou, W., Wu, L., Kang, L., Rizo, J., Zhang, R., Xu, T., & Ma, C. (2015). Syntaxin opening by the MUN domain underlies the function of Munc13 in synaptic-vesicle priming. *Nature Structural & Molecular Biology*, *22*(7), 547–554. https://doi.org/10.1038/nsmb.3038

Yao, J., Gaffaney, J. D., Kwon, S. E., & Chapman, E. R. (2011). Doc2 Is a Ca2+ Sensor Required for Asynchronous Neurotransmitter Release. *Cell*, *147*(3), 666–677. https://doi.org/10.1016/j.cell.2011.09.046

Yoshihara, M., Guan, Z., & Littleton, J. T. (2010). Differential regulation of synchronous versus asynchronous neurotransmitter release by the C2 domains of synaptotagmin 1. *Proceedings of the National Academy of Sciences*, *107*(33), 14869–14874. https://doi.org/10.1073/pnas.1000606107

Zhang, X., Chen, Y., Wang, C., & Huang, L.-Y. M. (2007). Neuronal somatic ATP release triggers neuron–satellite glial cell communication in dorsal root ganglia. *Proceedings of the National Academy of Sciences*, *104*(23), 9864–9869. https://doi.org/10.1073/pnas.0611048104

Zilly, F. E., Sørensen, J. B., Jahn, R., & Lang, T. (2006). Munc18-Bound Syntaxin Readily Forms SNARE Complexes with Synaptobrevin in Native Plasma Membranes. *PLoS Biology*, *4*(10), e330. https://doi.org/10.1371/journal.pbio.0040330